

# The diversity of planetary system architectures: contrasting theory with observations

Y. Miguel,<sup>1,2★</sup> O. M. Guilera<sup>1,2</sup> and A. Brunini<sup>1,2★†</sup>

<sup>1</sup>Facultad de Ciencias Astronómicas y Geofísicas, Universidad Nacional de La Plata, Paseo del Bosque s/n, La Plata (1900), Argentina

<sup>2</sup>Instituto de Astrofísica de La Plata (CCT La Plata-CONICET, UNLP), Paseo del Bosque s/n, La Plata (1900), Argentina

Accepted 2011 June 15. Received 2011 June 14; in original form 2010 October 5

## ABSTRACT

In order to explain the observed diversity of planetary system architectures and relate this primordial diversity to the initial properties of the discs where they were born, we develop a semi-analytical model for computing planetary system formation. The model is based on the core instability model for the gas accretion of the embryos and the oligarchic growth regime for the accretion of the solid cores. Two regimes of planetary migration are also included. With this model, we consider different initial conditions based on recent results of protoplanetary disc observations to generate a variety of planetary systems. These systems are analysed statistically, exploring the importance of several factors that define the planetary system birth environment. We explore the relevance of the mass and size of the disc, metallicity, mass of the central star and time-scale of gaseous disc dissipation in defining the architecture of the planetary system. We also test different values of some key parameters of our model to find out which factors best reproduce the diverse sample of observed planetary systems. We assume different migration rates and initial disc profiles, in the context of a surface density profile motivated by similarity solutions. According to this, and based on recent protoplanetary disc observational data, we predict which systems are the most common in the solar neighbourhood. We intend to unveil whether our Solar system is a rarity or whether more planetary systems like our own are expected to be found in the near future. We also analyse which is the more favourable environment for the formation of habitable planets. Our results show that planetary systems with only terrestrial planets are the most common, being the only planetary systems formed when considering low-metallicity discs, which also represent the best environment for the development of rocky, potentially habitable planets. We also found that planetary systems like our own are not rare in the solar neighbourhood, its formation being favoured in massive discs where there is not a large accumulation of solids in the inner region of the disc. Regarding the planetary systems that harbour hot and warm Jupiter planets, we found that these systems are born in very massive, metal-rich discs. Also a fast migration rate is required in order to form these systems. According to our results, most of the hot and warm Jupiter systems are composed of only one giant planet, which is also shown by the current observational data.

**Key words:** planets and satellites: formation.

## 1 INTRODUCTION

To date, the number of planetary systems discovered orbiting single stars, similar to the Sun, in the solar neighbourhood has increased to 315 (<http://exoplanets.org/>), of which 237 are apparently single-

planet systems, while the remaining 78 are multiple-planet systems. The first multiple planetary system discovered orbiting a single star is the one around 47 UMa, which to date harbours two confirmed planets of masses 2.5 and 0.5 Jupiter masses ( $M_J$ ) and semi-major axes 2.1 and 3.6 au (Butler & Marcy 1996; Fischer et al. 2002) and one inferred planet of  $1.6M_J$  located at 11.6 au from the central star (Gregory & Fischer 2010), which means that this planetary system hosts three giant planets located at distances greater than 1 au from the central star. On the other hand, another example is the system GJ 876, which houses four planets (two giant planets, one Neptune and one super-Earth) located at distances less than 1 au (Delfosse

★E-mail: ymiguel@fcaglp.unlp.edu.ar (YM); abrunini@fcaglp.unlp.edu.ar (AB)

†Member of the Carrera del Investigador Científico, Consejo Nacional de Investigaciones Científicas y Técnicas (CONICET).

et al. 1998; Marcy et al. 1998, 2001; Rivera et al. 2005, 2010). There are also examples of systems with a hot Jupiter and another giant planet, located away from the central star at a distance greater than 1 au, like the system HD 217107 (Fischer et al. 1999; Vogt et al. 2005). As shown in these examples, the planetary system population is remarkably diverse. It displays a wide range of architectures with properties that reflect the environment where they were born and the different mechanisms of formation and evolution, which are of special interest to test theoretical models of planetary system formation.

All the information provided by the observations of planetary systems has still not been analysed by theoretical models, although in recent years there have been a few works dealing with planetary system formation and evolution that intend to explain some of the observed trends of planetary systems, for example, the work of Thommes, Matsumura & Rasio (2008), who present self-consistent numerical simulations of planetary system formation and study specifically how the properties of a mature planetary system map to those of its birth disc. Ida & Lin (2010) developed a semi-analytical code for planetary system formation, where they include the effect of resonant capture between embryos during type I migration and the calculation of embryos' orbital and mass evolution after the gas depletion. Their aim was to show that the formation of super-Earths close to the star is possible and that they are more common than hot Jupiters. Nevertheless, answers to questions such as how common are planetary systems like our own in the solar neighbourhood? what factors influence the architecture of planetary systems? what are the differences and similarities between planetary systems? and what is the diversity of planetary systems expected to be found in the solar neighbourhood? remain uncertain.

With these questions in mind, our main objective is to explore the importance of several factors in defining the architecture of a planetary system. We also intend to explain the observed diversity of planetary systems and link them to their birth environment. We explore different gas and solid disc profiles, as well as different planetary migration rates, to find out which factors reproduce the different planetary systems observed. According to this, and based on the protoplanetary disc observational data, we predict the systems that are more common and thus expected to be found in the solar neighbourhood. In this way, we intend to unveil whether our Solar system is a rarity or whether more planetary systems like our own are expected to be found in the near future. We also analyse which is the more favourable environment for the formation of habitable planets.

Based on the most accepted scenario for explaining the formation of planetary systems, our semi-analytical model adopts the core instability model for giant planet formation. In this scenario, the mass distribution in the protoplanetary disc is important, since it defines the number and location of the final giant planets that would define the architecture of the planetary system. Thus, we consider a large range of disc sizes and masses according to recent protoplanetary disc observations (Andrews et al. 2009; Isella, Carpenter & Sargent 2009) and assume a nebula with a surface density profile motivated by similarity solutions for viscous accretion discs (Lynden-Bell & Pringle 1974; Hartmann et al. 1998), which is intended to be simple but is a computationally feasible description, consistent with protoplanetary disc observations. Our embryos start growing in the oligarchic growth regime (Kokubo & Ida 1998) and if they are able to accrete gas, their gaseous envelope will grow according to a prescription found from results obtained by Fortier, Benvenuto & Brunini (2009). As the embryos are embedded in a gaseous disc, we also include the effects of their

mutual interaction, considering type I and II regimes of planetary migration.

We found that those planetary systems that host small rocky planets are the most common in the solar neighbourhood. These 'low-mass planetary systems' are the only ones that form in a low-metallicity environment and represent the best site for the formation and development of terrestrial planets in the habitable zone. The final number of embryos that harbour these planetary systems is strongly dependent on the initial disc profile and migration rate assumed. Another striking result is that planetary systems similar to our Solar system are expected to be common in the solar neighbourhood. These systems are formed in massive discs, with no preferential areas for the accumulation of solids. Finally, we found that those planetary systems with only hot ( $a < 0.07$  au) and warm ( $0.07 < a < 1$  au) Jupiter planets need a very massive, metal-rich disc to be formed and also a fast migration rate. Our results are consistent with the observational trend and show that most of these systems harbour only one giant planet.

## 2 DESCRIPTION OF THE MODEL

We have developed a semi-analytical model for planetary system formation. This model was explained in detail in our previous work (Miguel, Guilera & Brunini 2011); in this section, we will summarize it for completeness.

### 2.1 Protoplanetary disc

The minimum-mass solar nebula (MMSN) model of Hayashi (1981) is usually used for modelling the protoplanetary nebula. As was explained in previous works (Davis 2005; Desch 2007; Miguel et al. 2011), this model suffers from multiple limitations. In order to avoid these limitations, we adopt a different model to represent the initial protoplanetary disc structure. Following Andrews et al. (2009), we assume that the gaseous surface density of the disc is

$$\Sigma_g(a) = \Sigma_g^0 \left( \frac{a}{a_c} \right)^{-\gamma} e^{-\left(\frac{a}{a_c}\right)^{2-\gamma}} \quad (1)$$

based on the works of Lynden-Bell & Pringle (1974) and Hartmann et al. (1998). In the equation,  $a_c$  is a parameter introduced to smoothly end the disc and is fitted from the observations, the  $\gamma$  exponent indicates how the material is distributed in the disc and  $\Sigma_g^0$  is a constant value, which is calculated from the disc's mass and also depends on the characteristic radius and the adopted disc profile.

In a similar way, the solid surface density distribution,  $\Sigma_s(a)$ , is

$$\Sigma_s(a) = \Sigma_s^0 \eta_{\text{ice}} \left( \frac{a}{a_c} \right)^{-\gamma} e^{-\left(\frac{a}{a_c}\right)^{2-\gamma}} \quad (2)$$

with  $\eta_{\text{ice}}$  a function which is 1/4 inside the snow line and 1 outside it, representing the change in the solids due to water condensation (Hayashi 1981; Weidenschilling et al. 1997; Mordasini, Aibert & Benz 2009).

We note that the relation between the gas and solid surface density distributions gives the abundance of heavy elements. For the case of a disc orbiting a star with metallicity [Fe/H], it is (Murray et al. 2001; Ida & Lin 2004b; Mordasini et al. 2009)

$$\left( \frac{\Sigma_s^0}{\Sigma_g^0} \right)_* = \left( \frac{\Sigma_s^0}{\Sigma_g^0} \right)_{\odot} 10^{[\text{Fe}/\text{H}]} = z_0 10^{[\text{Fe}/\text{H}]}, \quad (3)$$

where  $z_0$  is the primordial abundance of heavy elements in the Sun which was found to be  $z_0 = 0.0149$  by Lodders (2003). In this work,

we will assume that the stellar metallicities follow a lognormal distribution fitted from the results of the CORALIE sample (Santos et al. 2003).

Recent protoplanetary disc observations show that the exponent in the inner part of the disc ( $\gamma$ ) takes values between 0.4 and 1.1 (Andrews et al. 2009). Following these observations and the results of the comparison with the MMSN model, we explore three different values for this exponent:  $\gamma = 0.5, 1$  and  $1.5$ .

The sample of discs generated have masses that follow a log-Gaussian distribution fitted from recent protoplanetary disc observations (Andrews et al. 2009; Isella et al. 2009).

Since gravitational instabilities can occur in any region of the disc if it becomes cool enough or the mass distribution is really high, we check the stability of the discs generated. In the linear regime, the gravitational instability limit is given by the Toomre parameter (Toomre 1964)

$$Q = \frac{c_s k}{\pi G \Sigma_g} \quad (4)$$

with  $k$  the epicyclic frequency of the disc. When the discs are Keplerian,  $k = \Omega_k$  and the  $Q$  parameter is

$$Q \simeq 1.24 \times 10^5 \left( \frac{a}{1 \text{ au}} \right)^{\gamma - \frac{7}{4}} \left( \frac{a_c}{1 \text{ au}} \right)^{-\gamma} \left( \frac{M_\star}{M_\odot} \right) \frac{e^{\left(\frac{a}{a_c}\right)^2 - \gamma}}{\Sigma_g^0}, \quad (5)$$

where a value of  $Q \leq 1$  represents an unstable disc.

As shown in the equation, disc stability depends on the initial disc profile, so discs with the same mass could be stable or unstable depending on the value of  $\gamma$  adopted. Discs with  $\gamma = 0.5$  are more massive in the outer disc than those characterized by larger values of  $\gamma$ . As a consequence, discs with relatively small mass and  $\gamma = 0.5$  could develop gravitational instabilities, while discs with higher values of  $\gamma$  require a larger disc mass in order to undergo gravitational instabilities. As a result, we found that when the highest value of  $\gamma$  is considered ( $\gamma = 1.5$ ), there are discs with masses up to  $1 M_\odot$  that present values of  $Q > 1$  in the entire disc. These extremely massive discs should not be considered as Keplerian. In order to avoid these discs, we add another condition for stability. We assume that a disc is stable if  $Q > 1$  and its mass does not exceed 20 per cent of the mass of the central star (Hartmann et al. 1998; Klahr et al. 2006).

The location of the inner boundary of the dust disc was found by Vinkovic (2006) through observations of young stellar objects and is

$$a_{\text{in}} = 0.0688 \left( \frac{1500 \text{ K}}{T_{\text{sub}}} \right)^2 \left( \frac{L_\star}{L_\odot} \right)^{1/2} \text{ au} \quad (6)$$

with  $T_{\text{sub}}$  the dust sublimation temperature taken as 1500 K, and  $L_\star$  and  $L_\odot$  are the stellar and solar luminosities, respectively. Though Vinkovic (2006) found that this is the inner radius of the dust disc, we adopt this value to represent the end of both discs.

We locate one initial embryo at the inner radius and the others are separated by a distance  $\Delta a$  from each other until the end of the disc is reached. This outer edge is the one that contains 95 per cent of the total disc mass, so it is not always the same and as a result, the initial number of embryos,  $N_{\text{ini}}$ , will be different according to the disc initial properties. As was shown in our previous work (Miguel et al. 2011), the greater the mass of the disc, the lower the initial number of embryos. This is because the separation between the embryos of mass  $M_t$  is

$$\Delta a = 10 \left( \frac{2M_t}{3M_\star} \right)^{1/3} a. \quad (7)$$

The larger the initial mass of the embryo, the greater the separation, and as a result, massive discs have a lower  $N_{\text{ini}}$ .

Finally, our discs are not time-invariant. We model the evolution of the gaseous disc with a very simple exponential decay model, which empties the gaseous disc everywhere on time-scales between  $10^6$  and  $10^7$  yr in agreement with the observations of circumstellar discs (Haisch, Lada & Lada 2001; Hillenbrand 2006). The discs of solids change locally due to the accretion of the embryos.

## 2.2 The growth of the embryos

In the beginning, there are  $N_{\text{ini}}$  initial embryos embedded in a swarm of planetesimals in a gaseous disc. These embryos will grow due to the accretion of solids, gas and also due to mergers with other embryos.

The relative velocity between the embryo and the neighbouring planetesimals is an important factor in determining different regimes of embryo growth. Our model begins when the cores have enough mass to increase the velocity dispersion of the surrounding planetesimals, a fact which leads to a slow regime that will dominate the embryo growth. This is the oligarchic growth regime (Kokubo & Ida 1998).

The initial mass necessary for exciting the neighbouring planetesimals and turning on the oligarchic growth regime was found by Ida & Makino (1993) and is given by

$$M_{\text{oli}} \simeq \frac{1.6a^{6/5} 10^{3/5} m^{3/5} \Sigma_s^{3/5}}{M_\star^{1/5}}, \quad (8)$$

with  $m$  the effective planetesimal mass.

The solid accretion rate in this regime of growth depends on the radius ( $R_p$ ) and total mass of the planet and the velocity dispersion ( $\sigma$ ) which in turn depends on the planetesimals' eccentricity. Following Safronov (1969), the embryo eats planetesimals at the rate

$$\frac{dM_s}{dt} = 10.53 \Sigma_s \Omega R_p^2 \left( 1 + \frac{2GM_t}{R_p \sigma} \right), \quad (9)$$

where  $\Omega$  is the Kepler frequency. As the solid accretion rate depends on the planetesimals' eccentricity, we assume that they reached an equilibrium value due to the balance between the protoplanets' gravitational perturbations and the gas drag effect (Thommes, Duncan & Levison 2003). The accretion of solids ends when the solid surface density is equal to zero, which means that the embryos consume most of the planetesimals available in their feeding zone and scatter the others (Thommes et al. 2003; Ida & Lin 2004a).

Up to now we assume that the only mechanism for the growth of the embryos is the accretion of small planetesimals, but they can also grow due to collisions with other embryos. This is a very important effect from which most of the embryos suffer (Miguel & Brunini 2010), and determines their final characteristics. The giant impacts between embryos result in the merger of the cores and therefore represent a sudden and big increase in the mass of the embryo. We assume that when two cores are located at a distance less than 3.5 Hill radii, they will collide and merge (Chambers 2006; Wright et al. 2009).

Following Chambers (2006), we consider that when the embryos have enough mass to be able to retain a gaseous atmosphere, this gas increases the collision cross-section of the embryo and the solid accretion rate is enhanced. At first, this gaseous envelope is able to maintain hydrostatic equilibrium, but when the core reaches a critical mass, the envelope can no longer be maintained by hydrostatic equilibrium and the gas accretion on to the core begins

(Stevenson 1982; Ikoma, Nakazawa & Emori 2000). Following Ida & Lin (2004a), we assume a simplified formula for this critical mass given by

$$M_{\text{crit}} \sim 10 \left( \frac{\dot{M}_c}{10^{-6} M_{\oplus} \text{ yr}^{-1}} \right)^{1/4}. \quad (10)$$

The gaseous envelope contracts on its own, on a time-scale given by the following formula that we obtained by fitting the results of the self-consistent code developed by Fortier et al. (2009):

$$\frac{dM_g}{dt} = \frac{M_t}{\tau_g}, \quad (11)$$

where  $M_g$  is the mass of the surrounding envelope and  $\tau_g$  is its characteristic Kelvin–Helmholtz growth time-scale given by

$$\tau_g = 8.35 \times 10^{10} \left( \frac{M_t}{M_{\oplus}} \right)^{-4.89} \text{ yr}. \quad (12)$$

### 2.3 Orbital evolution of the embryos

While the embryos manage to form, they are embedded in a gaseous disc which interacts with the cores, leading to the orbital evolution of the embryos called planetary migration.

There are different regimes of planetary migration. We assume that our cores migrate due to type I and II planetary migration as explained in the following.

#### 2.3.1 Migration type I

This regime acts on low-mass planets, which are treated as a small perturbation, and the linearized hydrodynamic equations are solved for the disc response. This regime was studied by Goldreich & Tremaine (1980) and Ward (1997) and leads to an orbital motion of the embryos towards the central star. Following Tanaka, Takeuchi & Ward (2002), the migration rate is

$$\left( \frac{da}{dt} \right)_{\text{migI}} = c_{\text{migI}} (2.7 + 1.1\beta) \left( \frac{M_t}{M_{\star}} \right) \left( \frac{\Sigma_g a^2}{M_{\star}} \right) \left( \frac{a \Omega_k}{c_s} \right)^2 a \Omega_k, \quad (13)$$

where

$$\beta = - \frac{d \log(\Sigma_g)}{d \log(a)} = \gamma + (2 - \gamma) \left( \frac{a}{a_c} \right)^{2-\gamma} \quad (14)$$

as the time-scale for type I migration can be shorter than the disc lifetime, and the factor  $c_{\text{migI}}$  is introduced to consider effects that might stop or slow down migration (e.g. Menou & Goodman 2004; Nelson & Papaloizou 2004; Davis 2005; Masset et al. 2006; Kley, Bitsch & Klahr 2009; Paardekooper et al. 2010) without introducing a major degree of complexity into the model.

#### 2.3.2 Migration type II

In the presence of a very massive embryo, the problem can no longer be treated as linear and then the disc response should be treated as a non-linear case. This is the type II migration regime (Lin & Papaloizou 1985; Lin, Bodenheimer & Richardson 1996), which for a disc with a viscosity characterized by  $\alpha = 10^{-3}$  (Ida & Lin 2004a) is

$$\left( \frac{da}{dt} \right)_{\text{migII}} \simeq 3 \text{ sign}(a - R_m) \alpha \frac{\Sigma_g(R_m) R_m^2}{M_t} \frac{\Omega_k(R_m)}{\Omega_k} \left[ \frac{h(R_m)}{a} \right]^2 a \Omega_k(R_m), \quad (15)$$

where

$$R_m = 10e^{\frac{2r}{\tau_{\text{disc}}}} \text{ au}, \quad (16)$$

where  $\tau_{\text{disc}}$  is the gaseous disc depletion time-scale.

The embryos stop migrating when they reach the inner edge of the disc.

## 3 RESULTS

Our main objective is to know what are the typical composition and architecture that are expected to be found in a planetary system. To accomplish this goal and following earlier works of Ida & Lin (2004a), Miguel & Brunini (2009), Mordasini et al. (2009) and Miguel et al. (2011), we performed a series of Monte Carlo numerical simulations. We assume different unknown parameters, such as the density profile and the type I migration rate, in order to compare with the observations and find out what suits better the observational sample of planetary systems.

Following recent results of observations of protoplanetary discs (Andrews et al. 2009; Isella et al. 2009), we assumed that the exponent which characterizes the distribution of mass in the inner part of the disc adopts three values:  $\gamma = 0.5, 1$  and  $1.5$ . On the other hand, we suppose that the type I migration rate can be slowed down by 10–100 times, but we also analyse the cases where it is not delayed and where planetary migration is not considered.

Furthermore, we are also interested in finding out what are the parameters that link a planetary system with its birth disc and define the planetary system main characteristics. In order to study this problem, in each simulation, we generate 1000 planetary systems, where the initial conditions for each birth disc, taken at random, are as follows.

- (i) The time-scale for gas depletion has a uniform log distribution between  $10^6$  and  $10^7$  yr.
- (ii) The stellar mass has a uniform distribution in log-scale in the range of  $0.7$ – $1.4 M_{\odot}$ .
- (iii) The distribution of metallicities of solar-like stars in the solar neighbourhood follows a Gaussian distribution with  $\mu = -0.02$  and dispersion  $0.22$  (Mordasini et al. 2009).
- (iv) The total mass of the disc distribution is well approximated by a log-Gaussian distribution with mean  $-2.05$  and dispersion  $0.85$ . We obtained this value by assuming a log-Gaussian distribution and performing a non-linear least-squares fit to the sample observed by Andrews et al. (2009) and Isella et al. (2009).
- (v) The characteristic radius,  $a_c$ , is also well approximated by a log-Gaussian distribution with  $\mu = 3.8$  and  $\sigma = 0.18$ . This distribution was obtained with the same procedure as described in the previous item.

We want to know how many of these planetary systems generated in our simulations match with an observed one. Thus, with the aim of comparing with the observations, we assumed that an observed planetary system matches quantitatively with an artificial one when the masses and semi-major axes of its giant planets are the same to less than 10 per cent. To date, there are 315 planetary systems found orbiting a single star, similar to the Sun; 66 per cent of them could be reproduced quantitatively by our simulations. The remaining 33 per cent are multiple planetary systems, where we could not find artificial systems whose planets match exactly the mass and semi-major axis of those observed, although we have found qualitatively similar systems, which will be discussed in the next section, where we also analyse the different architectures found, the characteristics of the simulated planetary systems

**Table 1.** Percentage of the different planetary systems detected whose planets orbit around a single star with mass in the range  $0.7\text{--}1.4 M_{\odot}$ .

Types of planetary systems	Percentage of planetary systems detected
Hot and warm Jupiter systems	52.38
Solar systems	31.43
Cold Jupiter systems	0
Combined systems	16.19
Low-mass planetary systems	0

and how these final characteristics map the discs where they were born.

### 3.1 A new classification for planetary systems

So far, more than 300 planetary systems have been found orbiting a single star. These planetary systems present different characteristics, and after understanding their formation, composition and relation with their birth disc, it is appropriate to classify them according to their architecture.

Since most of the observed planets are giant planets, we use them for planetary system classification. In order to determine what mass is appropriate for separating planets into giant planets and low-mass planets, we look from the theoretical point of view. Planets with masses larger than  $\sim 15 M_{\oplus}$  have reached the crossover mass, which means that the runaway gas accretion process has begun. This process ends only when there is no residual gas in the disc or a gap forms near the planet's orbit, so planets with masses larger than  $15 M_{\oplus}$  are giant planets or failed giant planets (= Neptunes). These are the planets considered for our classification.

On the other hand, based on the observations, we note that these planets are located either near the central star (at distances less than 1 au), in an intermediate zone, or far away (at distances larger than 30 au), a fact that is the basis of our classification.

We then separate all the planetary systems according to the following classification.

(i) *Hot and warm Jupiter systems.* These planetary systems host planets with masses larger than  $15 M_{\oplus}$  at a distance less than 1 au.

(ii) *Solar systems.* A planetary system is an analogue of our Solar system if it harbours giant planets or Neptunes located between 1 and 30 au.

(iii) *Combined systems.* These planetary systems harbour at least one giant planet within 1 au and at least one in the middle part of the disc, between 1 and 30 au.

(iv) *Cold Jupiter systems.* If giant planets are located farther than 30 au, then they are cold Jupiter systems.

(v) *Low-mass planetary systems.* These systems have only planets with masses less than  $15 M_{\oplus}$ .

In Table 1, we show the statistics of the population of planetary systems observed. In order to compare with our population of artificial planetary systems, we eliminate from the observed sample those planetary systems formed around binary or multiple stars, as well as those where the mass of the central star is less than 0.7 or greater than  $1.4 M_{\odot}$ . The total number of observed planetary systems analysed in the table is 315.<sup>1</sup>

We note that most of the planetary systems are hot and warm Jupiter systems, but we also found a large percentage of planetary

system analogues to the Solar system, although these do not harbour planets like the Earth or are not detected yet. It must be noted that this sample is biased towards those planets that are easier to detect with current observational techniques, but we hope that in the near future planets like our own will be easier to detect and this will improve the statistics, but in the meantime, some predictions can be made about what we hope to find.

To this end, in the following, we will explore the statistics of the population of planetary systems found in our simulations. Tables 2, 3 and 4 show the percentage of different kinds of planetary systems found when assuming different initial disc profiles:  $\gamma = 0.5$ , 1 and 1.5, respectively. In each table, we show the statistics when different migration rates are considered. We perform simulations without migration and adopting different type I migration rates, which are indicated in the different columns.

*The first striking result is that in all cases, considering all discs ( $\gamma = 0.5$ , 1 or 1.5) and all the migration rates (without migration and when  $c_{\text{mig1}} = 0.01$ , 0.1 and 1), it is always the planetary systems with small planets which are in vast majority.* It means that these systems are in invisible majority, because none of them has been detected yet. However, if the observational techniques allow it, a lot of them would be detected and this is what we expect to find in the near future.

We also note that we found zero cold Jupiter systems in all the analysed cases. This is because the core instability model allows the formation of giant planets close to the star, the snow line being the preferred zone (Ida & Lin 2004a), which is believed to be initially located in the inner part of the disc. This model for planetary formation cannot explain the formation of planets as far as 30 au. Another possibility could be that the planet migrates outwards, which could occur if it shares a resonance with another giant planet and the inner planet is significantly more massive than the outer one (Crida, Masset & Morbidelli 2009). Finally, we should consider the possibility that the planet may have formed in the inner planetary system and then been ejected outwards. Nevertheless, none of these hypotheses is addressed in our study. Therefore, we need a different scenario to explain the origin of these giant planets, maybe a different mechanism of formation (see e.g. Boss 1997, 1998), or migration, or consider the formation and subsequent ejection of the planets towards the outer system (Chatterjee et al. 2008; Dodson-Robinson et al. 2009; Veras, Crepp & Ford 2009).

Finally, we point out that, as we note in Tables 2–4, there are failed planetary systems. These systems were born in very low mass discs, which did not allow the formation of objects with masses larger than planet Mercury's mass.

Table 2 shows the numerical results when  $\gamma = 0.5$  and, as shown in the table, when planetary migration is not considered, we found a large percentage of system analogues to our Solar system, while the percentage of hot and warm Jupiter systems is really small. This is because giant planets are formed in regions of higher accumulation of solids. The solid surface density profile considered in this case allows the formation of these planets only near the ice line, since there is no accumulation of material in other regions of the disc. In addition, if the migration is not considered, they stay where they were formed.

When the migration is considered, the planets have a radial motion that moves them towards the star and, as a consequence, the number of hot and warm Jupiter and combined systems increases. We also note that when migration is the fastest ( $c_{\text{mig1}} = 1$ ), the population of low-mass planetary systems increases, because in this case the time-scale for type I migration is really fast and inhibits the growth of embryos.

<sup>1</sup> <http://exoplanets.org/>

**Table 2.** Percentage of planetary systems formed when  $\gamma = 0.5$  and with different migration rates.

Types of planetary systems	$\gamma = 0.5$			
	No migration	$c_{\text{migl}} = 0.01$	$c_{\text{migl}} = 0.1$	$c_{\text{migl}} = 1$
Hot and warm Jupiter systems	0.2	2.7	4.3	4.1
Solar systems	11.3	12.6	9.1	1.8
Cold Jupiter systems	0	0	0	0.0
Combined systems	0	3	2.2	0.5
Low-mass planetary systems	77.2	70.8	73.4	81.9
Failed planetary systems	11.3	10.9	11	11.7

**Table 3.** Percentage of planetary systems formed when  $\gamma = 1$  and with different values of  $c_{\text{migl}}$ .

Types of planetary system	$\gamma = 1$			
	No migration	$c_{\text{migl}} = 0.01$	$c_{\text{migl}} = 0.1$	$c_{\text{migl}} = 1$
Hot and warm Jupiter systems	1.8	8.2	11.1	5.8
Solar systems	23.7	19.9	7.7	1.4
Cold Jupiter systems	0	0	0	0.0
Combined systems	0	9.3	6.3	0.3
Low-mass planetary systems	73.4	61.6	72.8	88.3
Failed planetary systems	1.1	1	2.1	4.2

**Table 4.** Percentage of planetary systems formed when  $\gamma = 1.5$  and with different values of  $c_{\text{migl}}$ .

Types of planetary systems	$\gamma = 1.5$			
	No migration	$c_{\text{migl}} = 0.01$	$c_{\text{migl}} = 0.1$	$c_{\text{migl}} = 1$
Hot and warm Jupiter systems	4.5	15.3	14.8	3.7
Solar systems	27.1	16.4	7.2	0
Cold Jupiter systems	0	0	0	0
Combined systems	0.9	15.6	6	0
Low-mass planetary systems	67.3	52.5	64.6	56.6
Failed planetary systems	0.2	0.2	7.4	39.7

Table 3 shows the statistics when we assume a surface density profile with an exponent that characterizes the inner part of the disc equal to 1. Assuming a sharper disc profile implies that the solids are accumulated in the inner regions of the disc. This accumulation allows the formation of a larger number of giant planets and as a result, the number of rocky and failed systems decreases, as shown in the table, in all the cases with the exception of the case where the parameter for delaying type I migration is equal to 1. As was said, this faster case inhibits the growth of the embryos, even for a  $\gamma = 1$  profile.

When we assume a profile with  $\gamma = 1.5$ , we found the results shown in Table 4. This case is characterized by a large accumulation of solids in the inner disc and a lower density in the outer region. Then, the population of low-mass planetary systems is still decreasing and the number of hot and warm Jupiter systems is still increasing, because the solid surface density is very high in the inner part of the disc, while it falls rapidly beyond the snow line, a fact that favours the formation of Jupiter planets inside 1 au, and, as a consequence, we found a larger percentage of hot and warm Jupiter systems in this case.

### 3.2 Characterizing different types of planetary systems

We divided the planetary systems into five classes and had a statistical overview of them, comparing with the observational data. In this section, we explore in detail each class of planetary systems.

#### 3.2.1 Hot and warm Jupiter systems

As shown in Table 1, 52.38 per cent of the planetary systems known so far are hot and warm Jupiter systems. This is because the hot Jupiters are easier to detect, but according to our results, this type of planetary system is not the most common in the solar neighbourhood.

Fig. 1 shows a comparison between some examples of hot and warm Jupiter systems detected and some systems artificially formed with our model. In the figure, we compare only the characteristics of the planets in the systems, not the stars. Also, when speaking of artificial systems, only the planets with masses larger than  $15 M_{\oplus}$  are plotted. This is because terrestrial planets evolve for  $\simeq 100$  to 200 Myr. During this time, the gravitational interactions between

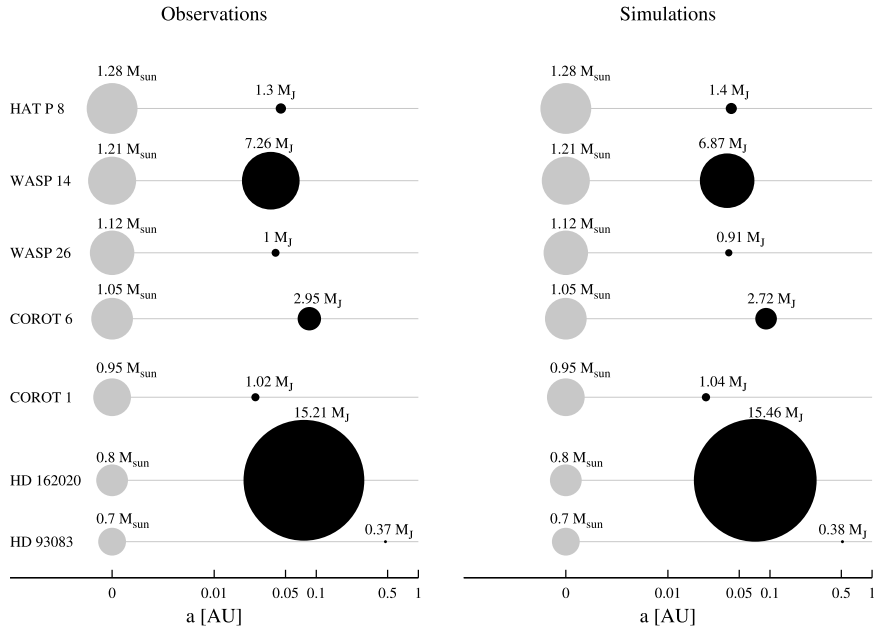


**Figure 1.** The figure shows some examples of hot and warm Jupiter systems with a single planet observed, shown in the first column, compared with similar hot and warm Jupiter systems generated in our simulations (second column). The semi-major axis is shown in the abscissa, while the size of the circle indicates the planet’s mass, which is also printed in Jupiter masses ( $M_J$ ) above each planet.

the embryos (after nebular gas was dissipated) play a fundamental role. In this work, we only considered the evolution of a system during 20 Myr and we did not take into account the gravitational interactions between the embryos. For these reasons, we consider that our results can only be compared with observations of giant exoplanets.

As shown in the figure, our model reproduces quantitatively the hot and warm Jupiter systems observed.

The observed systems, HAT-P-8 (first row), WASP-26 (third row) and HD 162020 (sixth row), are similar to artificial systems that were generated assuming a disc profile characterized by  $\gamma = 1$  and the fastest migration rate. The artificial systems generated in the second and fifth rows were formed considering a disc profile with  $\gamma = 1.5$  and also  $c_{\text{migl}} = 1$ . The system analogous to Corot 6 (fourth row) was formed when assuming  $\gamma = 1.5$  and a migration rate delayed by only 10 times and, finally, the system with the smallest hot Jupiter, shown in the last row, was formed under the assumption of a disc profile characterized by  $\gamma = 1.5$  and no migration.

As shown in the figures, with the exception of the last system, the others were formed assuming a disc profile characterized by a large accumulation of solids in the inner disc and the fastest migration rate assumed in this work. These are the preferred conditions for the formation of these systems. The artificial system generated in the seventh row is a rare system that was formed in a very massive disc where the solids are abundant in the inner disc ( $\gamma = 1.5$ ) and, as a consequence, a hot Jupiter *in situ* was allowed to form.

An analysis of observational data shows that there are 315 extrasolar planetary systems observed, of which 165 harbour giant planets located inside 1 au. Of these 165, 17 ( $\sim 10$  per cent) correspond to multiple systems, while the remaining are single planetary systems ( $\sim 90$  per cent). In order to determine whether this is a feature of these systems, we analyse the number of giant planets that are expected to be found in a system of this kind.

Fig. 2 shows histograms reproducing the percentage of artificial hot and warm Jupiter systems that harbour one, two or three giant

planets. Hot and warm Jupiter systems with more than three planets were not formed. The different rows show the results when different values of  $\gamma$  are considered. In the first row,  $\gamma = 0.5$ , in the second,  $\gamma = 1$ , and the last one shows the resulting histograms when  $\gamma = 1.5$ . The different columns show the results when different parameters for delaying type I migration are considered. In the first column, the migration was not considered, in the second column,  $c_{\text{migl}} = 0.01$ , in the third column,  $c_{\text{migl}} = 0.1$ , and the last column shows the histograms when the migration is not delayed.

We note that the number of giant planets that harbour a hot and warm Jupiter system is strongly dependent on the type I migration rate assumed. When the migration is not considered (first column), all the hot and warm Jupiter systems harbour only one giant planet. These are planets that were formed *in situ* and, as discussed in the previous section, these systems are very rare.

When migration is considered but delayed by 100 times (second column), there are hot and warm Jupiter systems which harbour two giant planets, but only those systems that were formed assuming a steeper disc profile ( $\gamma = 1$  or 1.5). A disc characterized by a profile with an exponent in the inner part given by  $\gamma = 1$  or 1.5 is a disc that favours the formation of giant planets, and because planets form closer to the star than when  $\gamma = 0.5$ , the migration pushes them towards the star and the system becomes a hot and warm Jupiter system.

In the third column, the migration is delayed by only 10 times, and we note that when the migration is faster, all the explored disc profiles form hot and warm Jupiter systems with two giant planets.

Finally, the last column shows the results when the migration is not reduced. We note that  $\gamma = 0.5$  is the only case when two giant planets are allowed to form. This is because the giant planets are formed farther from the central star than in the other cases, and although the fast migration inhibits the growth, they could grow by colliding with other embryos on their path. Nevertheless, in this case, the percentage of planetary systems with two giant planets is really small, less than 5 per cent. A fast migration

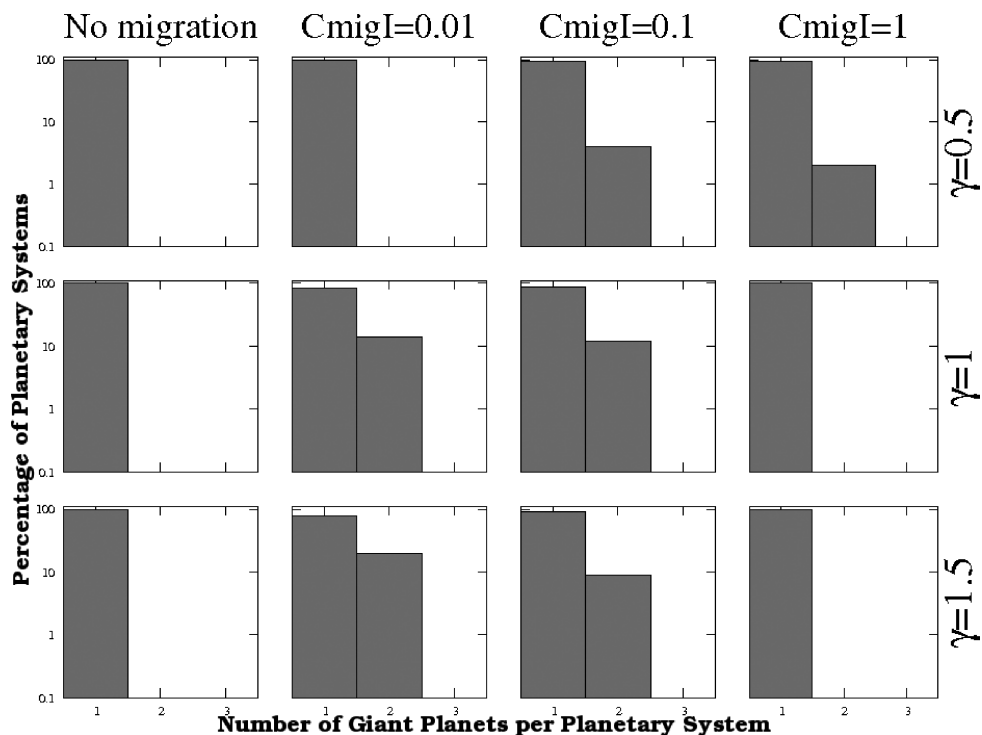


**Figure 2.** Histograms showing the number of giant planets per hot and warm Jupiter system. In the figure, the number of planets with masses larger than  $15 M_{\oplus}$  per planetary system is shown on the  $x$ -axis, and the  $y$ -axis shows the percentage of hot and warm Jupiter systems, which is shown in log-scale. The different rows show the resulting histograms for different values of  $\gamma$  and in the columns the results of assuming different type I migration rates are shown.

rate does not favour the formation of several giant planets either.

We see that such a fast migration inhibits the embryo's growth, which is why several giant planets in the same system are not allowed to form and as a result all the hot and warm Jupiter systems host only one giant planet.

As a general conclusion, we note that in all cases analysed, most of the hot and warm Jupiter systems are composed of only one giant planet, which is also shown by the current observational data (Wright et al. 2009).

### 3.2.2 Solar systems

So far, 99 of the observed planetary systems around single stars could be classified as solar systems. These 99 systems represent  $\sim 31.5$  per cent of all the planetary systems found, as shown in Table 1.

Fig. 3 shows a qualitative comparison between some examples of observed solar systems, which are shown in the first column and where only the giant planets are plotted, and some generated with our simulations, shown in the second column. In the figure, the semi-major axes of the planets are indicated on the  $x$ -axis, while their mass is represented with the different sizes of the black circles drawn above each planet. As shown in the figure, the observational sample of solar systems can be reproduced qualitatively by our simulations.

In the figure, the artificial solar system shown in the first row was formed considering  $\gamma = 1$  and  $c_{\text{migI}} = 0.1$ . In the second row, the solar system was generated assuming  $\gamma = 0.5$  and  $c_{\text{migI}} = 0.1$ . As shown in both cases, a flat disc is needed, in order to form these systems. This is because a small value of  $\gamma$  favours the formation of several giant planets farther from the central star. If a solar system

was born from a disc with a great accumulation in the inner disc, as is the case when  $\gamma = 1.5$ , which is also similar to the case of the MMSN model of Hayashi (1981), a very slow or zero migration is required in order for the giant planets formed in the ice line to stay there and not become hot Jupiters. That is precisely what is observed in the artificial system formed in the third row, which was generated assuming a disc profile characterized by  $\gamma = 1.5$  and where the planetary migration was not considered. Finally, the planetary system formed in the fourth row was born in a disc characterized by  $\gamma = 1$  and where the embryos do not migrate, which is consistent with the preferred scenario for the formation of these systems.

We cannot ignore our own Solar system, so a qualitative comparison of our planetary system with a generated one is shown in Fig. 4. The distance between the planets and their central star is shown on the  $x$ -axis and their mass is shown with the dark circles of different size, given for each planet.

In the figure, only Jupiter and Saturn are shown, because we do not find any artificial planetary system with the exact mass and location of all the giant planets in our Solar system. Then, the solar system shown in the figure harbours only two giant planets that match with our Solar system. For the formation of the artificial solar system, we assume that  $\gamma = 0.5$  and the planetary migration is not considered. As was said, a system with a very large value of  $\gamma$  does not favour the formation of several giant planets in the same system and is located farther away from the central star. On the other hand, a faster migration rate would locate the planets in the inner disc and the system would become a hot and warm Jupiter system. Thus, a small value of  $\gamma$  and a slow migration rate are the best conditions when trying to reproduce our Solar system.

Looking at the architecture of the 100 solar systems detected so far (where we include our Solar system), it can be noted that only



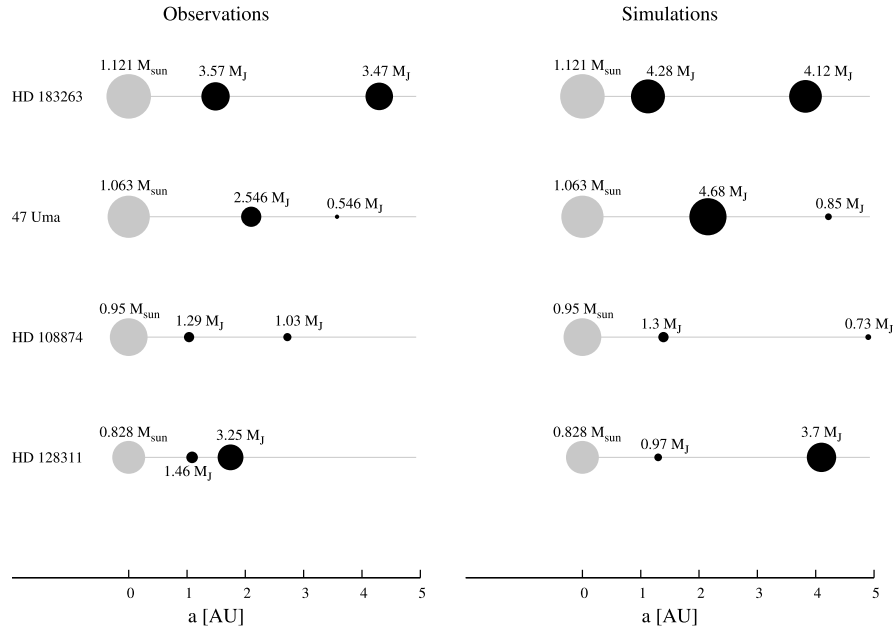


**Figure 3.** A sample of multiple solar systems observed, shown in the first column, compared to some examples generated in our simulations (second column). The position of a circle along the  $x$ -axis indicates the planet's location, while the size of the circle indicates their mass. The mass of the planet in  $M_J$  is indicated above each planet.

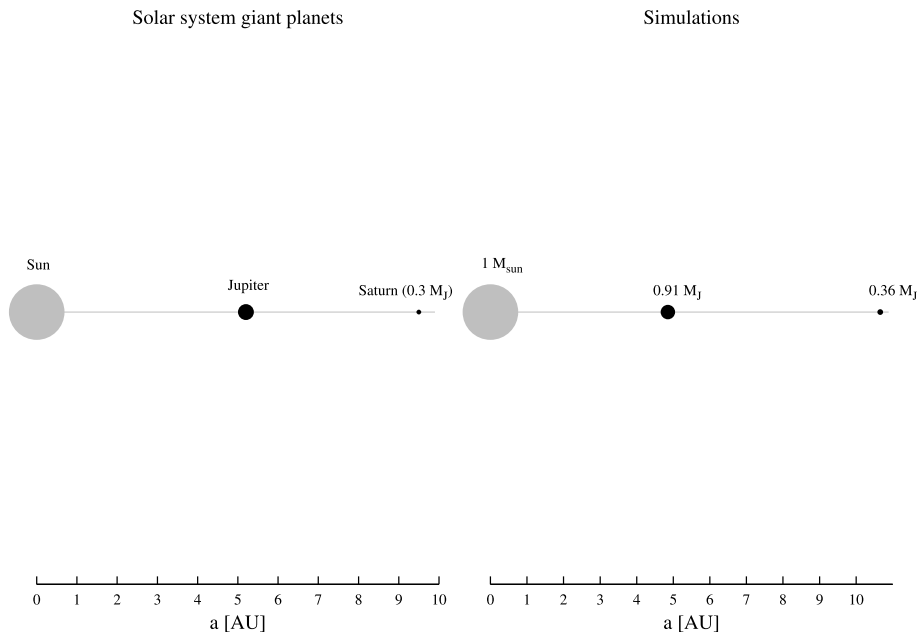


**Figure 4.** The figure shows a comparison between our Solar system (first column) and an artificial one generated with our simulations (second column). The semi-major axis of the planets is shown along the  $x$ -axis, while the size of the circle indicates their mass. The mass of the planets is indicated in  $M_J$ .

five of them have more than one giant planet and, with the exception of our Solar system, all of them harbour two giant planets. Since we do not know if this sample is representative of all solar systems or is due to an observational bias, we analyse statistically our numerical results.

Fig. 5 displays histograms showing the percentage of solar systems that harbour one, two or three planets with masses larger than  $15 M_{\oplus}$ . This figure is analogous to Fig. 2, where the columns show the results when different migration rates are considered and

the three rows show the results when different disc profiles are assumed.

The figure shows that solar systems with two giant planets are pretty common and those with three giant planets are very rare. This is because according to the core instability model a large amount of solid material is needed to form two giant planets. This allows rapid formation of very massive cores, which starts gas accretion, leading to the formation of giant planets. This usually occurs in the snow line region, which is the preferred formation zone for these planets.

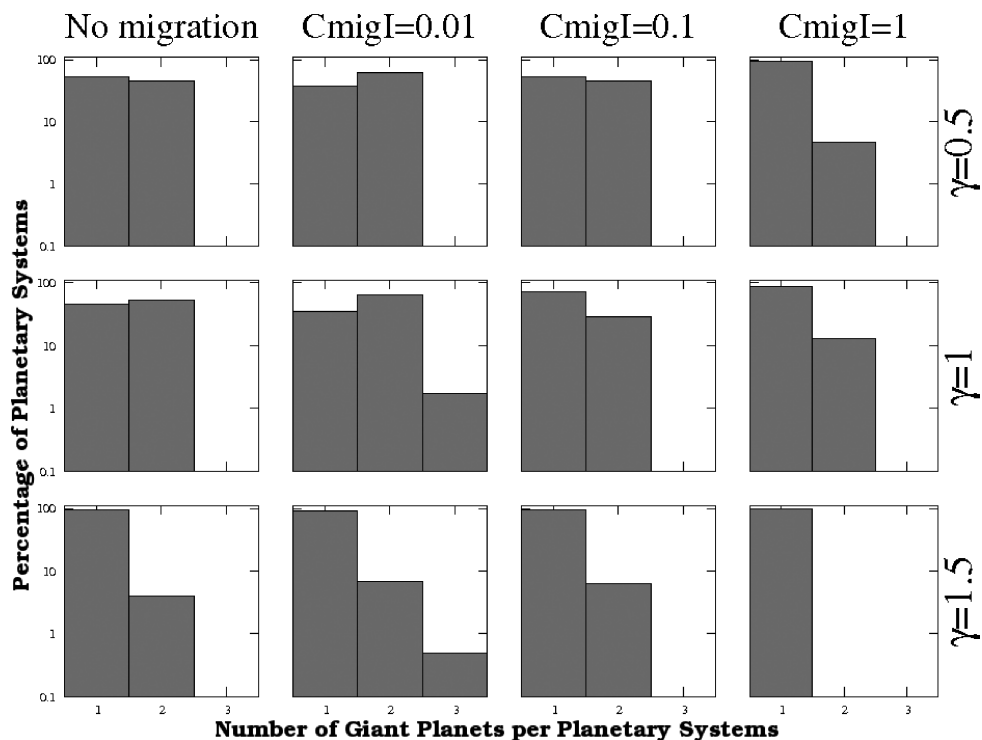


**Figure 5.** The figure shows histograms with the percentage of solar systems with one, two or three planets with masses larger than  $15M_{\oplus}$ . We present the results found with all the analysed cases, where the rows show the results found when different initial disc profiles are assumed ( $\gamma = 0.5, 1$  and  $1.5$ ) and the columns show the numerical results when we assume different migration rates,  $c_{\text{migI}} = 0, 0.01, 0.1$  and  $1$ .

If the disc is very massive and has a high metallicity, another giant planet could be formed, which does not occur in most cases.

The first row shows the results when the initial density profile of the disc is characterized by an exponent of  $\gamma = 0.5$ . The density profile in these discs is very smooth and there is no accumulation of gas and solids in the inner disc. As a consequence, the formation of giant planets may occur farther from the central star than in the case of steeper profiles. The migration moves them towards the star but it is not enough to locate them inside 1 au and for this reason these systems remain as solar systems. Since in this case the formation of several planets farther from the central star is favoured, in some cases, there are more solar systems with two giant planets than those formed with a single one.

When the density profile is a bit steeper,  $\gamma = 1$ , we note that there are still several planetary systems with two giant planets, even with three in some cases, so this disc profile also allows the formation of several giant planets per disc.

Finally, in the case of the steepest profile ( $\gamma = 1.5$ ), we see that the overall percentage of systems with multiple giant planets has fallen compared with previous cases, because a larger amount of solids in the inner part of the disc promotes the formation of a single giant planet per disc (Guilera, Brunini & Benvenuto 2010).

### 3.2.3 Combined systems

These systems represent an intermediate class between the hot and warm Jupiter systems and those analogous to the Solar system. Since belonging to this class implies the presence of at least one planet within 1 au and at least one outside, all these systems have two or more planets with masses greater than  $15M_{\oplus}$ . Our results agree with the observations regarding the frequency of these systems, although it could be a coincidence due to an observational bias. According

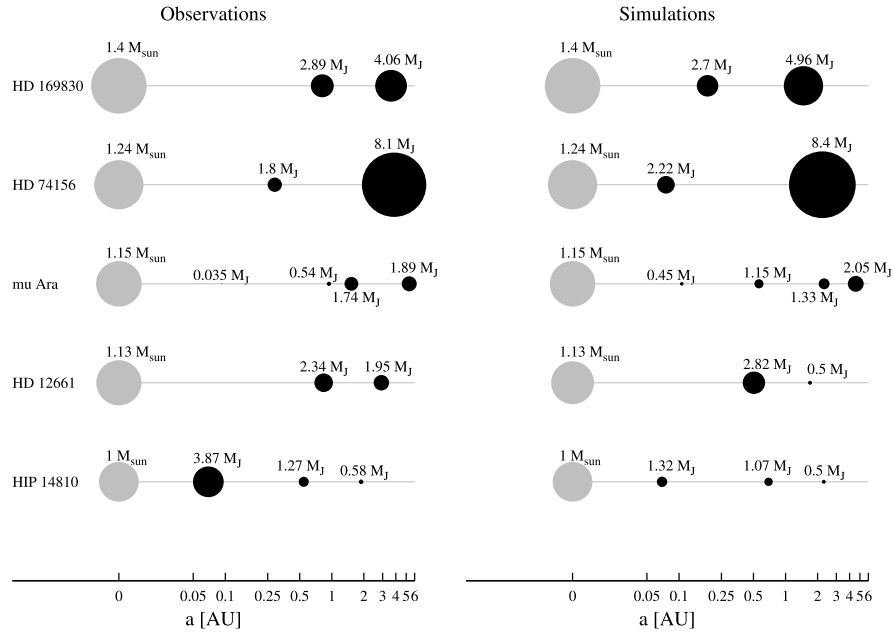
to the observations,  $\sim 16$  per cent of planetary systems discovered so far belong to this class, while our simulations show that in no case do combined systems generated exceed  $\sim 15$  per cent of the artificial sample.

Fig. 6 is analogous to Fig. 1, but in this case we show a comparison of combined systems.

As shown in the figure, the combined systems generated in our simulations match qualitatively with the observed systems, so that the architecture of these systems can be explained by the core accretion model and the current models of planetary migration. It is also noted that while these systems belong to the same class, they are qualitatively different, because multiple factors determine the final architecture of a planetary system. Some of these factors are the initial mass of the disc, the metallicity, the gaseous dissipation time-scale, the distribution of gas and solids along the disc and the migration time-scale.

The first row shows a system with two giant planets in which the mass of the inner planet is smaller than the mass of the exterior one. The artificial system was created with a disc characterized by a profile with  $\gamma = 1$  and a slow migration rate ( $c_{\text{migI}} = 0.01$ ). This system was formed in a disc with a smooth profile, where the more massive planet was formed in the region of greatest accumulation of solids (the snow line), while the lower mass planet was formed closer to the central star, inside the snow line. Since the migration was delayed by 100 times, these planets did not move too far from the region where they were born.

We also found systems such as the one shown in the second row, where the mass of the planets also grows outwards, but in this case the difference between the masses of the inner and outer planets is much greater than in the previous case. The artificial system was created with a profile characterized by  $\gamma = 1.5$  and slow migration ( $c_{\text{migI}} = 0.01$ ). This disc profile is characterized by



**Figure 6.** Examples of planetary systems observed (first column), compared to those generated in our simulations (second column), where only the giant planets were plotted. The position of a circle along the abscissa indicates the planet’s semi-major axis. The size of the circle indicates the planetary mass. In addition, the mass of the planet (in  $M_J$ ) is printed above each planet.

a great accumulation of solids in the inner disc, especially at the snow line, causing rapid formation of the most massive planet in this region. The lower mass planet was formed closer to the central star and as the profile allows a higher concentration of solids in the interior compared to the case of lower  $\gamma$  profiles, migration is also faster, so this planet migrates towards the star; on its path, it collides with other embryos and the mass of its core increases, being able to accrete gas before it is depleted, forming a large gaseous envelope.

The planetary systems shown in the third row also show that the mass grows outwards, but in this case, the systems harbour four planets with masses larger than  $15 M_{\oplus}$  and all of them have masses less than  $\approx 2M_J$ . The simulated system was generated assuming  $\gamma = 1$  and a migration rate faster than in previous cases ( $c_{\text{migr}} = 0.1$ ). The flat disc profile allows the formation of several giant planets in the same disc, but the growth is slower with this disc profile and the planets have smaller masses when compared to the previous case.

Finally, we found systems such as those shown in the fourth and fifth rows, where in both cases the mass grows inwards and the artificial systems were formed assuming a disc profile of  $\gamma = 1$  and a faster migration rate of  $c_{\text{migr}} = 0.1$ . In the case of the planetary systems generated in the fourth row, the most massive planet was born at the snow line and migrates inwards and the less massive planet was formed in the outer region with less gas and solids available to accrete. The system generated in the last row is a system where the embryos acquire most of their core mass due to collisions with other embryos. Then, the more massive planet migrates until the end of the disc and accretes more solids than the others.

We also noted that in the third and fifth rows, the systems were formed under identical parameters ( $\gamma = 1$ ,  $c_{\text{migr}} = 0.1$ ), but they have an opposite correlation of mass and distance. This implies that other factors must lead to this difference. The synthetic system in the third row was formed in a disc with  $M_d = 0.08 M_{\odot}$ ,  $a_c = 65$  au and a metallicity of 0.2. The system formed in the fifth row was born in a  $0.11 M_{\odot}$  disc,  $a_c = 47.85$  au and metallicity = 0.026. This means that the system in the fifth row had more solids and gas available

to form the giant planets. In this massive disc, the migration rate is faster (because of the larger amount of solids) and therefore the inner giant planet formed in the ice line and then migrated quickly, eating the other planets that might have formed there. In the meantime, the other giant planets formed farther from the star and migrated towards regions with a major solid surface density, growing in the process. On the other hand, the system in the third row has a lower disc mass and most importantly the characteristic radius is much larger compared with that in the previous case. This implies that the solids are spread over a much larger area and, as a consequence, the planetary migration was not so fast and the planets stayed where they were born. As a conclusion, we note that while the initial disc profile and the migration rate have a strong influence on the final architecture of the system, there are also other important parameters considered while defining it. This will be studied in Section 3.4.

### 3.2.4 Low-mass planetary systems

Low-mass planetary systems are those that do not host planets with masses larger than  $15 M_{\oplus}$ . Although none of these systems is observed yet, as shown in Tables 2–4, the majority of stars would not host giant planets, so this kind of planetary system represents a substantial fraction of planetary systems which are not deeply studied yet.

In the standard scenario of rocky planet formation, the final stage is the giant impact regime. With our model, we are able to study the first stages of rocky planet growth in the context of a disc where several cores are formed simultaneously. Studying the last stage of rocky planet growth implies a dynamic monitoring of phenomena such as resonant interactions during the last stages of their growth (e.g. Chambers 2001; Raymond et al. 2009), which are not analysed with our model. Nevertheless, we believe that our study is an important complement to numerical dynamical studies that analyse the last phases of growth, since we provide the initial conditions for these studies.

With the aim of analysing the final number of planets found in a low-mass planetary system as a function of the initial mass of the protoplanetary disc ( $M_d$ ), we divide the planetary systems into three types and analyse the final number of planets found per system in each class.

The first group are those low-mass planetary systems formed in low-mass discs ( $M_d < 0.05 M_\odot$ ), which are the most common low-mass planetary systems. The second group are those formed in intermediate-mass discs ( $0.05 \leq M_d < 0.1 M_\odot$ ) and the last group are the ones originated in very massive discs ( $M_d \geq 0.1 M_\odot$ ), which are the less common systems that are characterized by small metallicities. These low-mass planetary systems formed in very massive discs are most common when the migration rate is faster, because it inhibits the growth of the embryos.

Fig. 7 shows histograms representing the final number of embryos per planetary system. These plots were made based on the results found when the planetary migration is not considered. In the figure, the solid line shows the histogram for those planetary systems formed from a low-mass disc, the grey dotted line represents the histogram for the systems that were born in an intermediate-mass disc and the black dotted line is the resulting histogram for very massive discs. As the planetary system evolution is different when assuming different values for the  $\gamma$  exponent, Fig. 7(a) shows the results when  $\gamma = 0.5$ , Fig. 7(b) shows the histograms resulting when  $\gamma = 1$ , and when  $\gamma = 1.5$ , we found the results shown in Fig. 7(c).

The most massive discs have a lower initial number of embryos because the separation between them is larger. This implies that, in massive discs, embryos must be more massive in order to collide with a neighbouring core. When the disc profile is characterized by an exponent in the inner disc given by  $\gamma = 0.5$ , it is a rather flat disc and the growth slows down much more on the inside than it increases on the outside, when compared to discs with a larger  $\gamma$ . As a result, the final number of embryos in these discs is greater than the number reached in low-mass discs, as could be seen in Fig. 7(a). We note in the figure that most of the planetary systems formed in massive discs have between 20 and 25 final embryos, while those formed in low-mass discs have between 10 and 20 rocky planets at the end of the simulation.

When the profile is a bit steeper,  $\gamma = 1$ , this trend continues (Fig. 7b), but when the disc is characterized by a density profile of gas and solids with an exponent in the inner region of  $\gamma = 1.5$ , the growth of the embryos is really fast, so the merger between the embryos is more frequent, and as a result, the final number of embryos in massive discs is smaller than the final number in low-mass discs (Fig. 7c).

As shown in Figs 7(a)–(c), the final number of embryos is strongly dependent on the initial disc profile. Nevertheless, this is not the only important factor, but we are also interested in the effect of planetary migration on the final number of embryos. Fig. 8 shows the final number of planets per planetary system, when considering different migration rates and disc profiles. The columns represent different type I migration rates, where the first column shows the simulation results when  $c_{\text{migl}} = 0.01$ , the second column shows the resulting histogram when the migration was delayed 10 times and the last column represents the histograms when  $c_{\text{migl}} = 1$ . The histograms in different rows are the simulation results when different initial disc profiles are assumed (in the first  $\gamma = 0.5$ , in the second  $\gamma = 1$  and in the last one  $\gamma = 1.5$ ).

The interaction between an embryo and the surrounding gas moves the embryo towards the central star. This produces a higher number of collisions and the result of these mergers will be a smaller

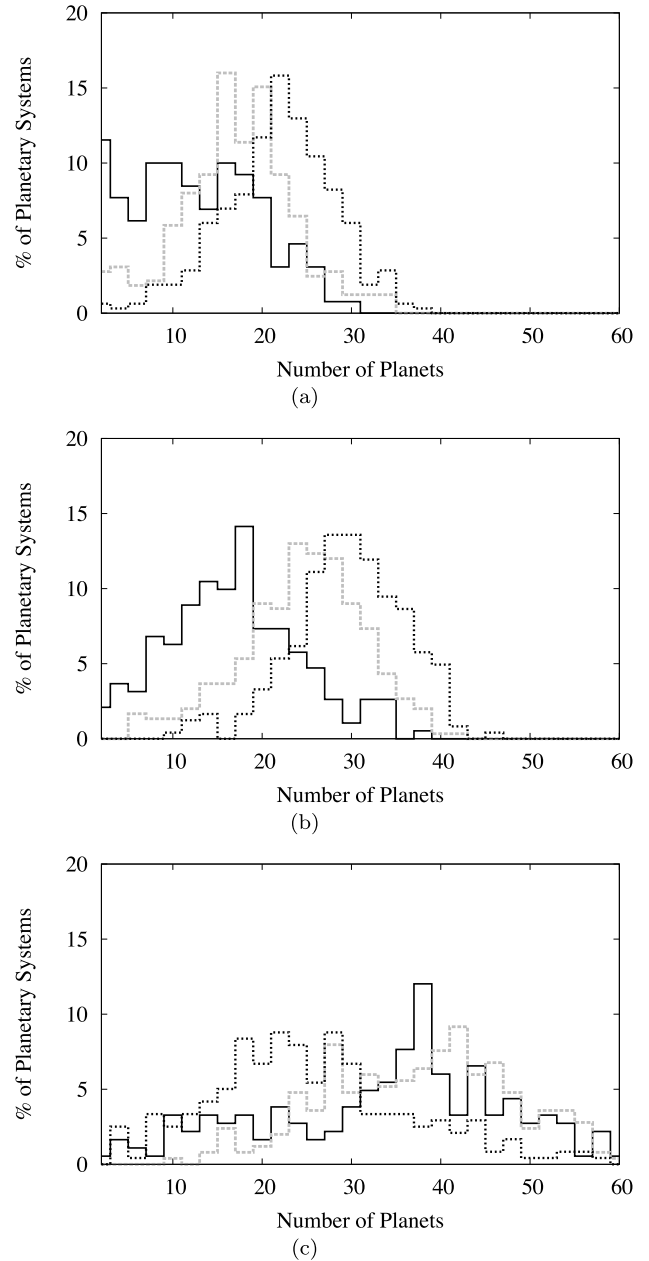


**Figure 7.** Histograms showing the number of planets per low-mass planetary system, where the planetary migration was not considered. Panel (a) shows the results when we consider  $\gamma = 0.5$ , panel (b) shows the percentage of planetary systems with a certain number of planets when  $\gamma = 1$  and, finally, the results obtained with  $\gamma = 1.5$  are shown in panel (c). In each figure, the solid line represents low-mass planetary systems formed in low-mass discs, the grey dotted line shows the histogram for those formed in intermediate-mass discs and the black dotted line shows the histogram for planetary systems formed from a massive disc.

number of embryos at the end of the simulation. While this effect is important in determining the final number of embryos per planetary system, the migration rate depends on the disc profile, and as we note in previous figures, the separation between the embryos also depends on the value of  $\gamma$  adopted, so the final number of embryos depends not only on the migration rate considered, but also on the initial disc profile.

When considering a profile characterized by  $\gamma = 0.5$ , we note that when  $c_{\text{migl}} = 0.01$  the histogram is similar to the case without

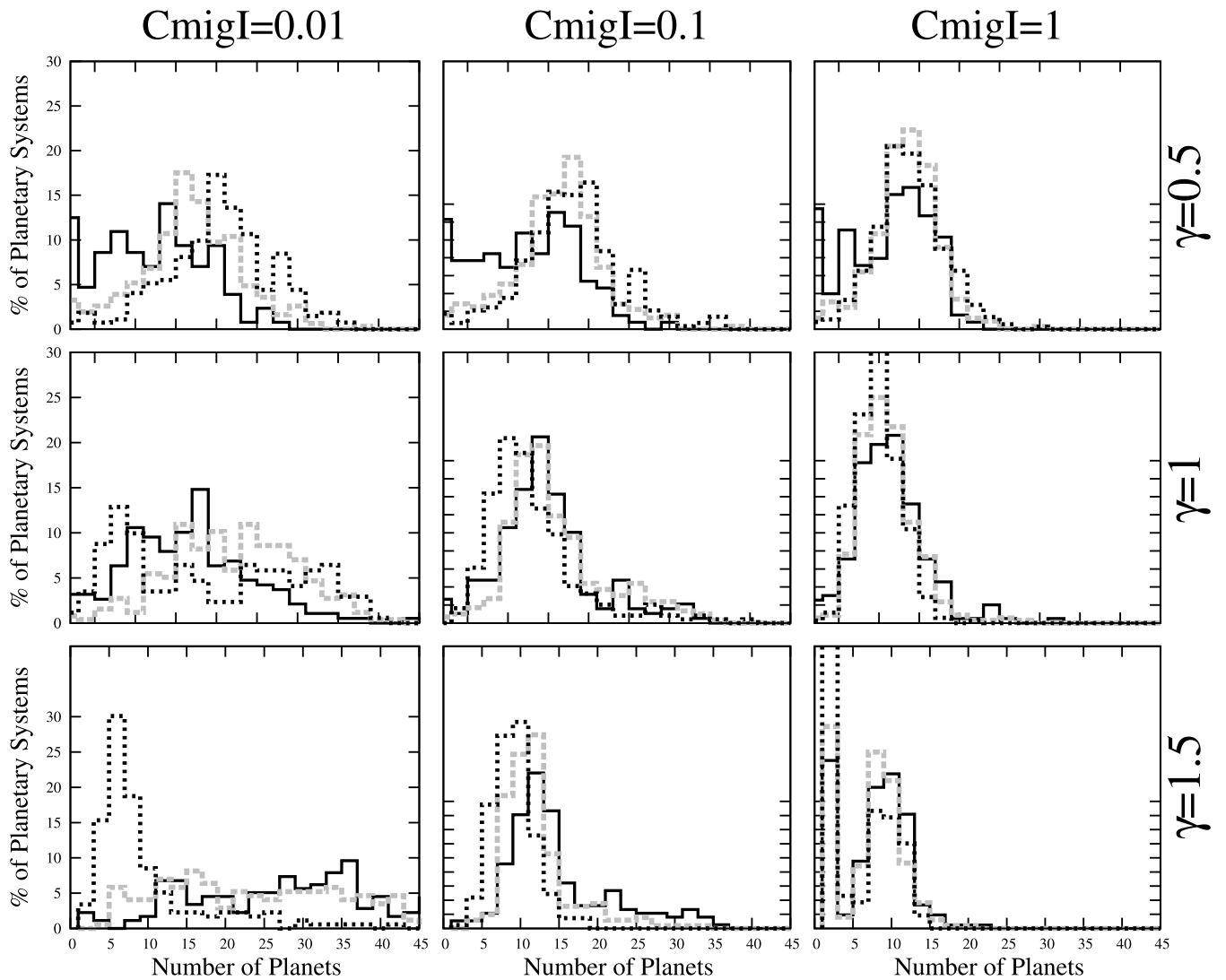


**Figure 8.** The figure shows histograms which represent the number of planets harboured per low-mass planetary system. In each histogram, the simulation results are separated into three categories: planetary systems formed in low-mass discs (solid line), planetary systems formed in intermediate-mass discs (grey dotted line) and planetary systems formed in massive discs (black dotted line). The rows show the results found when different initial disc profiles are assumed ( $\gamma = 0.5, 1$  and  $1.5$ ) and the columns show the numerical results when we assume different migration rates,  $c_{\text{migI}} = 0.01, 0.1$  and  $1$ .

migration, although in this case the majority of planetary systems formed in very massive discs host  $\sim 20$  planets. When the migration is faster,  $c_{\text{migI}} = 0.1$ , we note that the majority of planetary systems harbour between 15 and 20 final planets and when the migration is not delayed, most of the planetary systems harbour fewer than 15 planets at the end of the simulation.

When the initial disc profile is characterized by  $\gamma = 1$  and  $c_{\text{migI}} = 0.01$ , we note that the majority of planetary systems formed from less massive discs harbour between 15 and 20 final planets, while most of the low-mass planetary systems formed from very massive discs end up with a number of planets between five and 10. When the migration rate is faster, the disc mass is less important and most of the systems (formed from any disc) harbour fewer than 15 planets at the end of the simulation. Finally, when the migration is not slowed down, we see that the majority harbour fewer than 10 planets at the end of the simulation (20 million years).

The last row shows the histograms resulting when  $\gamma = 1.5$ . In this case, we note that even slow migration ( $c_{\text{migI}} = 0.01$ ) causes most of the systems formed from very massive discs to harbour

five planets at the end of the simulation. On the other hand, the number of final planets formed in systems with low-mass discs remains larger. When the migration is faster ( $c_{\text{migI}} = 0.1$ ), most of the planetary systems formed from any disc host 10 planets at the end of the simulation. Finally, when  $c_{\text{migI}} = 1$  we observe that most of the systems formed in intermediate- and low-mass discs harbour between five and 10 planets, while the vast majority of systems formed in very massive discs harbour fewer than five planets at the end of the simulation. This is a consequence of fast planetary migration. The migration is still more effective when the disc mass and solid surface density are higher, which is the case in this figure.

### 3.3 Habitable planets

Considerations of stellar flux and planet climate lead to the definition of the habitable zone as the region where an Earth-like planet could support liquid water on its surface (Kasting, Whitmire & Reynolds 1993). According to this definition, for the range of stellar masses considered in this work, the habitable zone lies between 0.9 and

**Table 5.** Percentage of planetary systems formed when  $\gamma = 0.5$ , and with different migration rates, that host habitable planets.

Types of planetary systems	$\gamma = 0.5$			
	No migration	$c_{\text{migl}} = 0.01$	$c_{\text{migl}} = 0.1$	$c_{\text{migl}} = 1$
Hot and warm Jupiter systems	0	0	0	0.1
Solar systems	2.8	1.4	0.7	0.4
Combined systems	0	0	0	0
Low-mass planetary systems	2.5	0.5	1.9	8.1

**Table 6.** Percentage of planetary systems formed when  $\gamma = 1$ , and with different migration rates, that host habitable planets.

Type of planetary systems	$\gamma = 1$			
	No migration	$c_{\text{migl}} = 0.01$	$c_{\text{migl}} = 0.1$	$c_{\text{migl}} = 1$
Hot and warm Jupiter systems	0	0	0.2	0.2
Solar systems	22.1	9.1	0.5	0
Combined systems	0	0	0	0
Low-mass planetary systems	38.7	19.7	14	9.5

**Table 7.** Percentage of planetary systems formed when  $\gamma = 1.5$ , and with different migration rates, that host habitable planets.

Type of planetary systems	$\gamma = 1.5$			
	No migration	$c_{\text{migl}} = 0.01$	$c_{\text{migl}} = 0.1$	$c_{\text{migl}} = 1$
Hot and warm Jupiter systems	0	0.4	0.3	0.2
Solar systems	22	3.4	0.4	0
Combined systems	0	0.1	0	0
Low-mass planetary systems	59.2	25.3	9.2	2.6

1.1 au. However, the evolution of Earth-like habitable planets is a complex process and locating a planet in the habitable zone is no guarantee of its habitability.

Although the potential habitability of an Earth-like planet depends on many factors, such as the tidal heating (Barnes et al. 2009; Jackson, Barnes & Greenberg 2009), its geophysical environment and atmospheric evolution (Lammer et al. 2010), the host star's activity and the planet's intrinsic magnetic field (Khodachenko et al. 2009), it is possible that planets in the habitable zone may contain water and host some life form. For this reason, missions that search for exoplanets intend to find small planets located in the habitable zone and the characterization of the stars and planetary systems that harbour them is important (Borucki et al. 2009; Kaltenegger et al. 2010).

On the other hand, gas giant planets are far easier than terrestrial planets to detect around other stars, and most of the planetary systems detected so far are formed mostly by giant planets. Should we continue to monitor these systems in the search for planets like the Earth or does the presence of a gas giant planet inhibit the formation of a small planet in the habitable zone? When speaking of hot and warm Jupiter systems, it is fairly clear that a migrating giant planet will cause any pre-existing low-mass planets or planetesimals at smaller radii to be lost, either by accretion or by scattering. What is not clear is whether a subsequent generation of planetesimals could form from the remnant disc after the giant path or whether rocky planets formed farther out in the disc subsequently migrate inwards and locate at smaller radii and perhaps in the habitable zone.

Recent studies dealing with these issues present varying results. On the one hand, Armitage (2003) developed a simple model for the evolution of gas and solids in the disc and analysed what remains

after a massive planet migration. He found that the replenishment of solid material in the inner disc following giant planet inward migration is generally inefficient and would not allow the formation of the second generation of habitable planets. On the other hand, Mandell, Raymond & Sigurdsson (2007) investigated the dynamics of post-migration planetary systems, considering only one giant planet migrating, and found that terrestrial accretion can occur during and after giant planet migration. This issue is not settled yet and depends on many factors, such as the time-scale of gas dissipation and the rates of accretion and planetary migration.

With our model, we are not able to analyse the subsequent formation of small planets, but we can analyse if it is possible that Earth-like planets formed at larger radii could end in the habitable zone due to subsequent migration. According to our model, when a giant planet migrates towards the star, the smaller embryos found on its path are accreted or scattered into external orbits. According to this, if we find an Earth-like planet located in the habitable zone in a hot and warm Jupiter system, then this means that it was born at a larger radius (farther than the giant planet formation zone) and a subsequent migration had located it in the habitable zone.

Tables 5–7 show the percentage of the planetary systems found in our simulations that host planets with masses less than  $15 M_{\oplus}$ , located between 0.9 and 1.1 au, in all the cases analysed.

As shown in the tables, there are very few hot and warm Jupiter systems where a subsequent migration located low-mass planets in the habitable zone. Since the higher the density of gas in the disc, the faster the migration rate, those discs with softer density profiles require a faster migration rate in order to move low-mass planets into the habitable zone. For this reason, when  $\gamma = 0.5$ , habitable planets are only found in hot and warm Jupiter systems

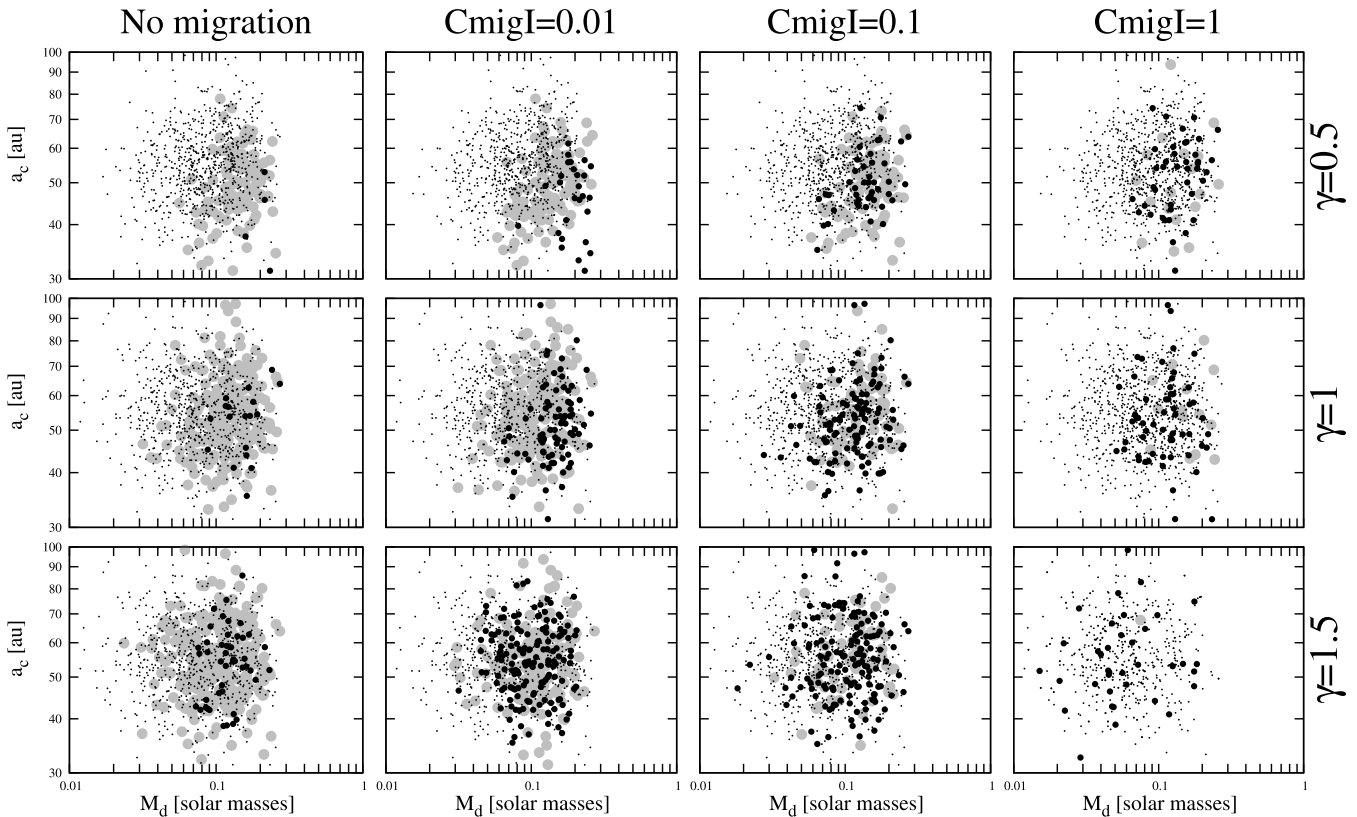


**Figure 9.** In the figure, each point represents a planetary system with a characteristic disc mass  $M_d$  and  $a_c$ . Planetary systems analogous to our Solar system are shown as big grey dots, hot and warm Jupiter systems are shown as big black dots and the small black dots are low-mass planetary systems. Each row shows the results when different values for  $\gamma$  are considered: in the first row  $\gamma = 0.5$ , in the second row  $\gamma = 1$  and in the third row  $\gamma = 1.5$ . The different columns represent different migration rates: the first column shows the results when  $c_{\text{migI}} = 0$ , the second column shows the results when  $c_{\text{migI}} = 0.01$ , the third column shows the results when  $c_{\text{migI}} = 0.1$  and the last one shows the resulting planetary systems when the migration rate is not delayed ( $c_{\text{migI}} = 1$ ).

when  $c_{\text{migI}} = 1$ . When the disc density profile is sharper ( $\gamma = 1$ ), low-mass planets in the habitable zone are found also when  $c_{\text{migI}} = 0.1$  and when  $\gamma = 1.5$ , there are planets that reach the habitable zone even for a migration rate as slow as in the case which was delayed by 100 times.

On the other hand, we note that low-mass, potentially habitable planets are found preferably in planetary system analogous to ours and also in low-mass planetary systems. These are the most favourable environments for the development of habitable planets.

### 3.4 Mapping the planetary system to its birth disc

One of the key questions regarding planetary systems is how their properties reflect the conditions of their parent nebula. There are many key parameters that play a role in defining the architecture of a planetary system. Here we explore the relevance of the initial disc mass, characteristic radius, metallicity, time-scale of gas disc dissipation, disc density distribution and migration rate.

#### 3.4.1 Disc mass and characteristic radius

The mass of the disc and how it is distributed through the disc determines the material available for the growth of embryos. A low-mass disc will form low-mass planetary systems, while a massive disc will favour the formation of planetary systems with giant planets.

The characteristic radius and exponent  $\gamma$  of the density profile are important because they indicate where most of the disc mass

is distributed. A disc with a large  $a_c$  and small value of  $\gamma$  is more extended and allows the formation of cores farther from the central star, but since the mass is distributed over a larger radius in a flat disc, mass concentration is not favoured and therefore the frequency of giant planetary formation decreases.

Fig. 9 shows the initial disc mass versus the characteristic radius of the disc, where each point represents a planetary system and we show the resulting planetary systems in all the cases considered in this work. The big grey dots are planetary systems analogous to our Solar system, the big black dots are the hot and warm Jupiter systems and the small black dots show the low-mass planetary systems. We noted that both the characteristic radius and the mass of the disc come from certain distributions, as discussed in Section 3. This fact is folded into the graphics and should be taken into account.

According to our results shown in the figures, in the case of a disc with a profile characterized by an exponent  $\gamma = 0.5$  on the inside (shown in the first row of graphs), a mass of at least  $0.06 M_{\odot}$  is needed to allow the formation of solar systems, and their formation is favoured when considering a slow migration rate. We also note that in this case there are very few hot and warm Jupiter systems when the migration is slow and it increases when considering faster migration rates, but anyway, a mass of at least  $0.1 M_{\odot}$  is needed in order to allow the formation of this kind of system. We note, however, that in the case of a migration rate delayed only 10 times, there are some systems that become hot and warm Jupiter systems with small initial discs, so a rapid migration rate allows the formation of these systems even for a relatively

small  $M_d$ . It is also pointed out that in general, the formation of hot and warm Jupiter systems and solar systems occurs preferably with a quite small  $a_c$ , which is due to the fact that a lower  $a_c$  favours the concentration of gas and solids and therefore the formation of giant planets.

In the second row, we show the resulting planetary systems when  $\gamma = 1$  is considered. In this case, the disc presents a larger density of solids and gas in the inner disc and as a result a mass of  $\sim 0.04 M_\odot$  is enough to form solar systems and there is no preferential  $a_c$  to allow the formation of these systems. A larger population of hot and warm Jupiter systems is found even when the migration is not acting, which implies that there are some initial discs which allow for the *in situ* formation of these planets, but they are very rare.

Finally, in the last row, the planetary systems are found when  $\gamma = 1.5$  is considered, where we note that these discs, which present a high abundance of gas and solids in the inner part, allow the formation of hot and warm Jupiter systems and solar systems even when the disc mass  $M_d \sim 0.02 M_\odot$  and for all  $a_c$ .

In general, it can be noted that the disc mass has a huge influence on defining the planetary system architecture, while the characteristic radius of the disc is not generally a relevant factor.

### 3.4.2 Stellar metallicity

Precise spectroscopic studies biased towards high-metallicity stellar samples (Fischer & Valenti 2005), those surveys that monitor stellar samples with low metallicities (Sozzetti et al. 2009) and other results

with no bias (Santos et al. 2004) have demonstrated that stars with giant planets tend to be particularly metal rich when compared to the average local field dwarfs.

The physical mechanism for these correlations is of particular interest. One possible explanation could be that a high-metallicity protostellar cloud forms a metal-rich star and disc, and as an increased surface density of solids would facilitate the growth of embryonic cores, gas giant planet formation is greatly enhanced around more metal rich stars. Alternatively, enhanced stellar metallicity may be a by-product of late-stage accretion of gas-depleted material and then a high-metallicity star does not necessarily imply that the initial disc was rich in solids.

Most of the evidence available suggests that the metallicity excess has a ‘primordial’ origin (Pinsonneault, DePoy & Coffee 2001; Santos, Israelian & Mayor 2001; Sadakane et al. 2002; Santos et al. 2003), and for this reason, we assume that a metal-rich star implies metal-rich discs, and thus the metal content of the cloud giving birth to the star and planetary system is indeed a key parameter to form a giant planet and determine the architecture of the planetary system.

Ida & Lin (2004b) studied through numerical simulations the giant planet formation in metal-rich discs. They found that since the solid accretion rate increases with the surface density of dust in the disc, the formation of gas giants tends to be more prolific in a metal-rich environment. Other authors find similar results (Kornet et al. 2005; Matsuo et al. 2007). Our results support this idea, but we also extend this study to the role of high metallicities in the diversity of planetary systems. In Fig. 10, each dot represents a

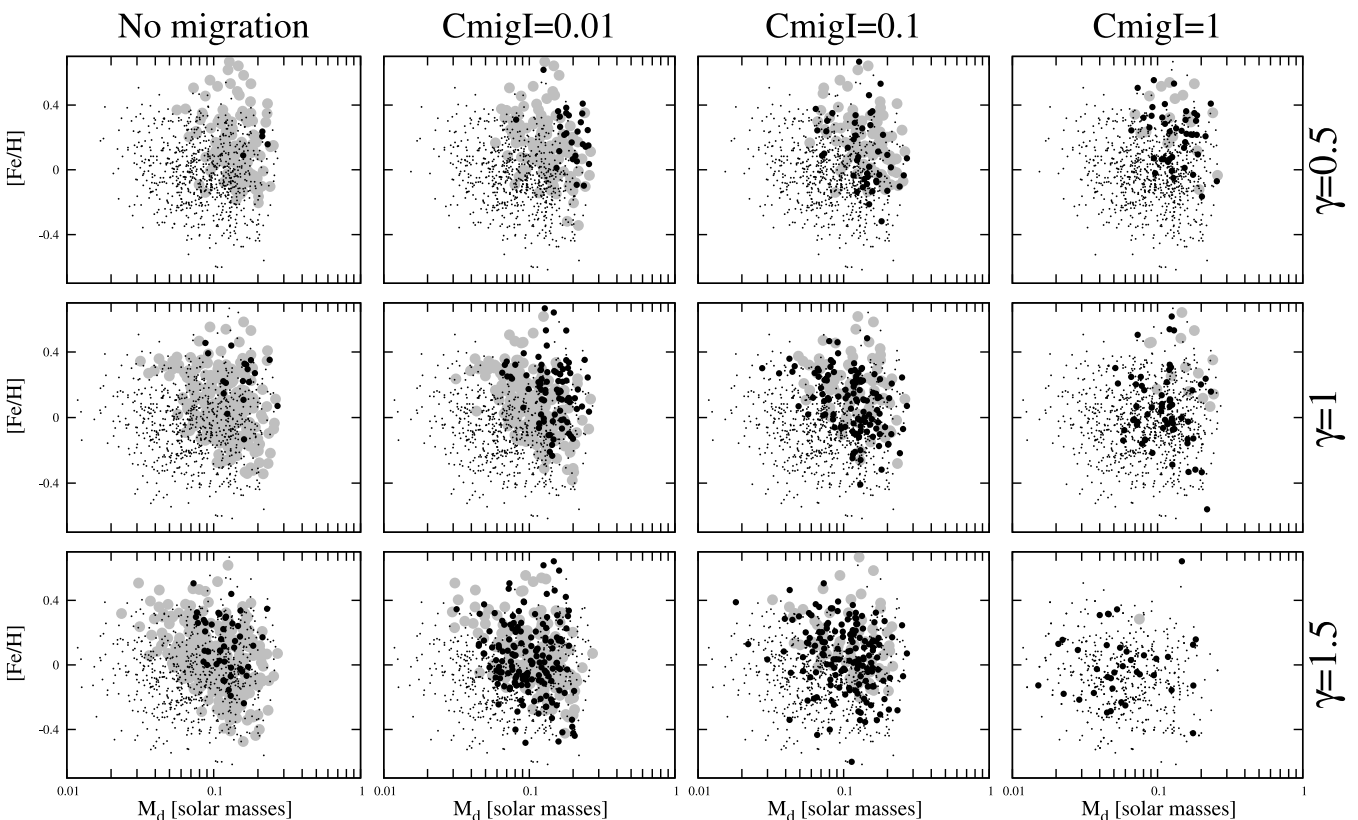


**Figure 10.** The resulting planetary systems with a characteristic disc mass and metallicity are plotted in the figures. The big grey dots represent the solar systems, the big black dots are hot and warm Jupiter systems and the small black dots are low-mass planetary systems. Different columns show the resulting planetary systems when different migration rates are considered: in the first column  $c_{\text{migI}} = 0$ , in the second column, the migration rate was delayed by 100 times, in the third column,  $c_{\text{migI}} = 0.1$  and in the last column,  $c_{\text{migI}} = 1$ . The different rows show the results when the disc density has a profile characterized by different values of  $\gamma$ . The results found when  $\gamma = 0.5$  are shown in the first row, when  $\gamma = 1$  in the second row, and when  $\gamma = 1.5$  in the last row.



planetary system (grey dots are the solar systems, big black dots are hot and warm Jupiter systems and small black dots are low-mass planetary systems), with a characteristic disc mass and stellar metallicity. The rows show the resulting planetary systems for the different density profiles considered in this work and the columns show the results with different migration rates.

As shown in the figures, when  $\gamma = 0.5$  (first row), a massive disc also needs a metallicity of at least  $-0.2$  in order to form solar systems and it has to be larger than  $-0.1$  to allow the formation of hot and warm Jupiter systems. Then, a massive disc is not the only important feature when forming planetary systems with giant planets; a high-metallicity disc is also needed. There are planetary systems formed in massive discs, but as they are characterized by low metallicities, they were not able to form giant planets and remained as low-mass planetary systems.

When  $\gamma = 1$ , the density profile is steeper, which allows the formation of solar systems and hot and warm Jupiter systems at lower metallicities. In this case, the lower limit for solar system formation is  $-0.5$  and the formation of hot and warm Jupiter systems is allowed when  $[\text{Fe}/\text{H}] \geq -0.4$ .

Finally, in the last case, when  $\gamma = 1.5$ , the solid surface density profile of the disc is the sharpest and this leads to a large concentration of solids in the inner disc, which allows the formation of hot and warm Jupiter systems even for discs with metallicities of  $-0.5$ , while the lower limit for allowing the formation of solar systems is almost  $-0.6$ .

A general result that we found is that in most of the low-metallicity discs, low-mass planetary systems are the most common systems, independently of the disc mass. This result could be in agreement with the results of the spectroscopic analysis done by Santos et al (2003) and also with the results of surveys biased to low-metallicity stars, which do not find giant planets on stars with low metallicities (Sozzetti et al. 2009). Nevertheless, we note that these observational results could mean that there are low-mass planets around all these stars which are not yet detected (which is in agreement with our results) or that these stars have no planets at all.

We also note that the higher the value of  $\gamma$ , the lower the metallicity limit for allowing the formation of giant planets. As a conclusion, a density profile characterized by  $\gamma < 1.5$  is in better agreement with the observations.

### 3.4.3 Depletion of the gas disc

Loss of the gaseous component of protoplanetary discs is due to a combination of the accretion on to the central star (Hartmann et al. 1998) and photoevaporation, that is, escape of the gaseous disc as a result of the illumination by external (Johnstone, Hollenbach & Bally 1998) or internal (Hollenbach et al. 1994) ionizing radiation.

According to observations in protoplanetary discs, the time-scale for the depletion of the gaseous component ranges between 1 and 10 million years (Haisch et al. 2001; Hillenbrand 2006). This time-scale is a key parameter in planetary system formation because it sets a limit for the end of gas giant formation, affects the environment for terrestrial planet formation and determines the planetary migration as well.

Fig. 11 is an analogue to Fig. 10, but in this case the gaseous disc characteristic time-scale versus disc mass is plotted.

We note that when the density profile is  $\gamma = 0.5$  (first row), there is no accumulation of solids in the disc, which leads to a lower accretion rate, and the time-scale for the depletion of the gaseous disc

is essential in determining the architecture of a planetary system. As a result, we note that a low disc mass combined with a faster depletion of the gaseous disc leads to low-mass planetary systems. On the other hand, a high disc mass combined with a slow depletion of the gas leads to solar systems and hot and warm Jupiter systems.

When  $\gamma = 1$  and  $1.5$  (second and third rows, respectively), the solid surface density profiles are steeper and as a result solids accumulate in the inner disc, promoting the rapid formation and migration of giant planets. Therefore, in this case of rapid formation, the gas dissipation time-scale is not a relevant parameter in defining the architecture of the planetary system.

These results are in agreement with those previously found by Thommes et al. (2008) who performed numerical simulations with a self-consistent code with the aim of addressing how the properties of a mature planetary system map to those of its birth disc. To this end, they performed simulations covering a range of disc parameters and generated 100 planetary systems. Regarding the relevance of the gaseous disc dissipation time-scale, they found similar results to ours, but with a more detailed code.

## 4 SUMMARY AND CONCLUSIONS

The ensemble of more than 300 planetary systems discovered orbiting single stars displays a wide range of architectures that show the diversity of planetary systems. This diversity is related to the environment where the planets were formed and evolved.

In order to study this diversity of extrasolar planetary systems, in this work, we have developed a semi-analytical code for computing planetary system formation which is based on the core instability model for the gas accretion of the embryos and the oligarchic growth regime for the accretion of the solid cores.

As our model is based on the core instability model, the mass distribution in the protoplanetary disc is important, since it defines the number and location of the final giant planets that would define the architecture of the planetary systems. Following protoplanetary disc observations, we explore different models for the initial protoplanetary nebula structure. Based on the similarity solutions for a viscous accretion disc, we assume that the gas and solid surface density are characterized by a power law in the inner part of the disc, with an exponent  $\gamma$  which takes the values  $\gamma = 0.5, 1$  and  $1.5$ , and an exponential decay in the outer part.

In our model, we also assume that the embryos have an orbital evolution due to their interaction with the gaseous disc which leads to type I and II planetary migration. Type I is very fast and a factor for delaying this migration rate is assumed, in order to represent the effects that could slow down or even stop it. We assume that the migration rate is delayed 10–100 times and also analyse the cases where it is not delayed, and in some simulations, the migration is not considered.

With this model, we perform 12 simulations, and in each one, we explore the three different gas and solid disc density profiles considered and also the different planetary migration rates. In each simulation, 1000 planetary systems are formed, whose initial conditions (mass and size of the disc, metallicity, mass of the central star and time-scale of gaseous disc dissipation) are taken randomly from distributions generated according to recent observational data.

We analyse this artificial sample statistically, comparing with the observed planetary systems. We also present a new classification of planetary systems based on the location of giant planets and characterize each class exploring how they reflect the disc where

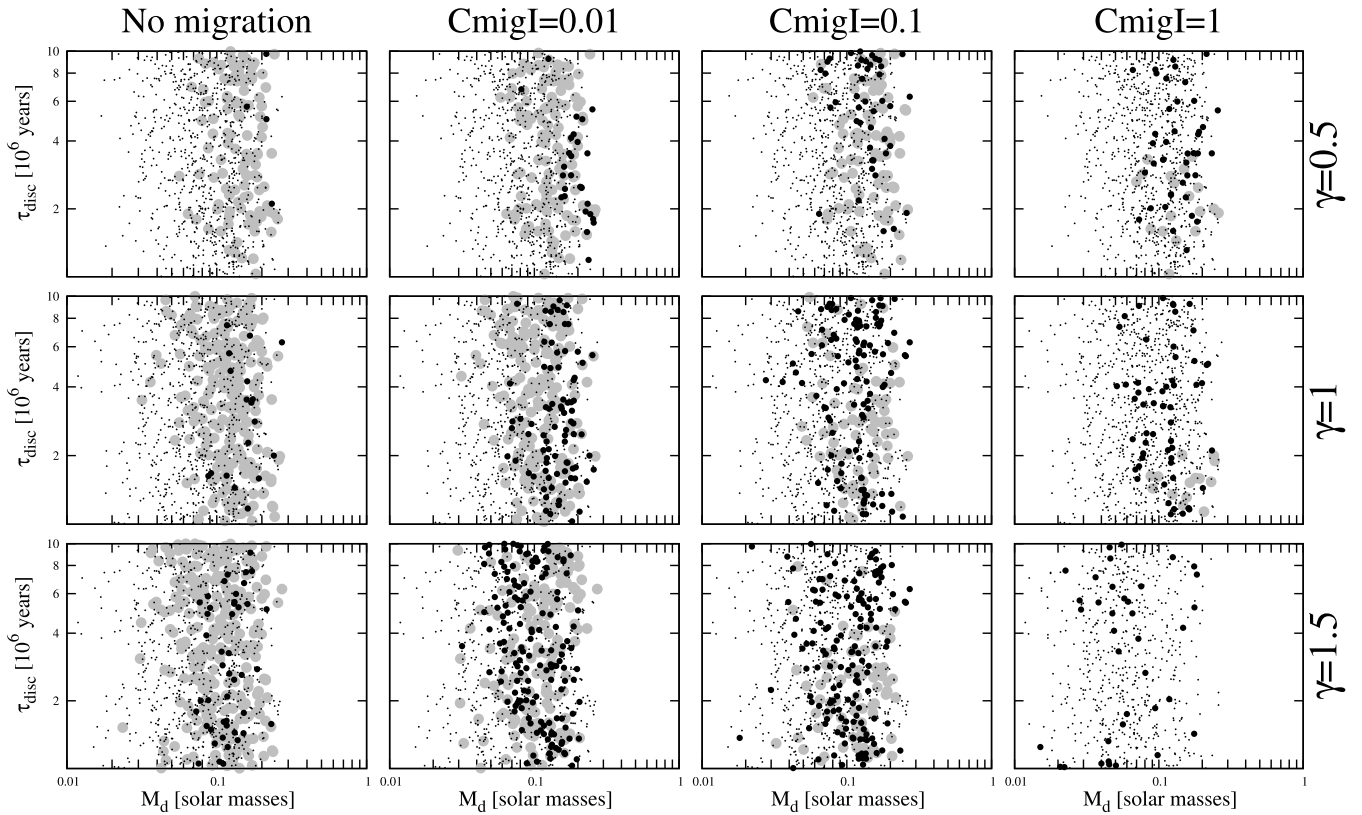


**Figure 11.** The figure shows the dependence of the time-scale for the depletion of the gaseous disc on the disc mass  $M_d$ , for all the planetary systems found. In this plot, the grey big dots represent the solar systems, the black big dots are the hot and warm Jupiter systems and the small black dots show low-mass planetary systems. The different columns represent the simulation results for different migration rates: the first column shows the results when the migration was not considered, the second column shows the results when the migration rate is delayed by 100 times, in the third column, the type I migration was delayed by 10 times and the last column shows the results when the migration is not delayed. The different rows represent the results when assuming different initial disc profiles:  $\gamma = 0.5, 1$  and  $1.5$ , respectively.

they were born, analysing the importance of key factors, such as the disc size and mass, stellar metallicity, gas depletion time-scale and planetary migration rate. We show the main characteristics of each class and the number of giant planets that we expect to find in those systems which harbour giant planets, and also the final number of small planets expected per low-mass planetary system. Finally, we analyse what are the best environments for the formation of small, potentially habitable planets and in which class of planetary systems they are expected to be found.

One of the striking results is that in all cases analysed, planetary systems with small planets are in vast majority when considering low-metallicity discs, being the only planetary systems formed in this case, when compared with those formed while considering solar-metallicity discs. Low-mass planetary systems are also the preferred planetary systems formed when a low-mass disc is combined with a faster depleting gaseous disc, the result also found by Thommes et al. (2008). The final number of embryos per planetary system is strongly dependent on the initial disc profile and migration rate assumed.

Planetary systems analogous to our Solar system are preferentially formed in massive discs, in a high-metallicity environment and where the disc profile that defines the gas and solid density in the inner disc is small. In addition, it also requires that the migration rate is not too fast, in order to avoid the planets being pushed towards the inner edge of the disc. We found solar systems with more than one giant planet, even with three, but in no case with more than three giant planets.

Assuming the sharpest disc profile, characterized by the largest value of  $\gamma$  assumed in this work, implies that the solids are accumulated in the inner regions of the disc, while they fall rapidly beyond the characteristic radius of the disc. This accumulation in the inner disc favours the formation of hot Jupiter planets, which are preferably formed in very massive discs combined with a slow depletion of the gas and a metal-rich environment. Also a fast migration rate is required in order to form these systems. According to our results, most of the hot and warm Jupiter systems are composed of only one giant planet, which is also shown by the current observational data.

We did not find any planetary system with giant planets located farther than 30 au, which is a consequence of the scenario assumed for giant planet formation.

We also analysed which are the most favourable environments for the formation of low-mass, potentially habitable planets and found that they are preferably formed in planetary systems analogous to our Solar system and also in low-mass planetary systems, which are the best environments for the development of these systems.

## ACKNOWLEDGMENTS

We thank an anonymous referee for useful comments that helped to improve our work.

## REFERENCES

Andrews S. M., Wilner D. J., Hughes A. M., Qi Ch., Dullemond C. P., 2009, *ApJ*, 700, 1502

- Armitage P. J., 2003, *ApJ*, 582, 47
- Barnes R., Jackson B., Greenberg R., Raymond S. N., 2009, *ApJ*, 700, 30
- Borucki W. et al., 2009, in Pont F., Sasselov D., Holman M., eds, *Proc. IAU Symp. 253, Transiting Planets*. Cambridge Univ. Press, Cambridge, p. 289
- Boss A., 1997, *ApJ*, 483, 309
- Boss A., 1998, *ApJ*, 503, 923
- Brunini A., Benvenuto O., 2008, *Icarus*, 194, 800
- Butler R. P., Marcy G. W., 1996, *ApJ*, 464, 153
- Chambers J., 2001, *Icarus*, 152, 205
- Chambers J., 2006, *Icarus*, 180, 496
- Chatterjee S., Ford E. B., Matsumura S., Rasio F. A., 2008, *ApJ*, 686, 580
- Crida A., Masset F., Morbidelli A., 2009, *ApJ*, 705, 148
- Davis S., 2005, *ApJ*, 627, 153
- Delfosse X., Forveille T., Mayor M., Perrier C., Naef D., Queloz D., 1998, *A&A*, 338, 67
- Desch S., 2007, *ApJ*, 671, 878
- Dodson-Robinson S. E., Veras D., Ford E. B., Beichman C. A., 2009, *ApJ*, 707, 79
- Fischer D. A., Valenti J., 2005, *ApJ*, 622, 1102
- Fischer D. A., Marcy G. W., Butler R. P., Vogt S. S., Apps K., 1999, *PASP*, 111, 50
- Fischer D. A., Marcy G. W., Butler R. P., Laughlin G., Vogt S. S., 2002, *ApJ*, 564, 1028
- Fortier A., Benvenuto O. G., Brunini A., 2009, *A&A*, 500, 1249
- Goldreich P., Tremaine S., 1980, *ApJ*, 241, 425
- Gregory P. C., Fischer D. A., 2010, *MNRAS*, 403, 731
- Guilera O. M., Brunini A., Benvenuto O. G., 2010, *A&A*, 521, 50
- Haisch K. E., Lada E. A., Lada C. J., 2001, *ApJ*, 553, 153
- Hartmann L., Calvet N., Gullbring E., D'Alessio P., 1998, *ApJ*, 495, 385
- Hayashi C., 1981, *Prog. Theor. Phys. Suppl.*, 70, 35
- Hillenbrand L. A., 2006, in Livio M., ed., *STScI Symp. Ser. 19, A Decade of Discovery: Planets Around Other Stars*, arXiv:astro-ph/0511083
- Hollenbach D., Johnstone D., Lizano S., Shu F., 1994, *ApJ*, 428, 654
- Ida S., Lin D. N. C., 2004a, *ApJ*, 604, 388
- Ida S., Lin D. N. C., 2004b, *ApJ*, 616, 567
- Ida S., Lin D. N. C., 2010, *ApJ*, 719, 810
- Ida S., Makino J., 1993, *Icarus*, 106, 210
- Ikoma M., Nakazawa K., Emori E., 2000, *ApJ*, 537, 1013
- Isella A., Carpenter J. M., Sargent A. I., 2009, *ApJ*, 701, 260
- Jackson B., Barnes R., Greenberg R., 2008, *MNRAS*, 391, 237
- Johnstone D., Hollenbach D., Bally J., 1998, *ApJ*, 499, 758
- Kaltenegger L. et al., 2010, *Astrobiology*, 10, 103
- Kasting J. F., Whitmire D. P., Reynolds R. T., 1993, *Icarus*, 101, 108
- Khodachenko M. L., Lammer H., Lichtenegger H. I. M., Grießmeier J.-M., Holmström M., Ekenbäck A., 2009, in Strassmeier K. G., Kosovichev A. G., eds, *Proc. IAU Symp. 259, Cosmic Magnetic Fields: From Planets, to Stars and Galaxies*. Cambridge Univ. Press, Cambridge, p. 283
- Klahr H., Rozyczka M., Dziourkevitch N., Wunsch R., Johansen A., 2006, in Klahr H., Brandner W., eds, *Planet Formation*. Cambridge Univ. Press, Cambridge, p. 42
- Kley W., Bitsch B., Klahr H., 2009, *A&A*, 506, 971
- Kokubo E., Ida S., 1998, *Icarus*, 131, 171
- Kornet K., Bodenheimer P., Rozyczka M., Stepinski T. F., 2005, *A&A*, 430, 1133
- Lammer H. et al., 2010, *Astrobiology*, 10, 45
- Lin D. N. C., Papaloizou J. C. B., 1985, in Black D. C., Matthews M. S., eds, *Protostars and Planets II*. Univ. Arizona Press, Tucson, p. 981
- Lin D. N. C., Bodenheimer P., Richardson D., 1996, *Nat*, 380, 606
- Lodders K., 2003, *ApJ*, 591, 1220
- Lynden Bell D., Pringle J. E., 1974, *MNRAS*, 168, 603
- Mandell A. M., Raymond S. N., Sigurdsson S., 2007, *ApJ*, 660, 823
- Marcy G. W., Butler R. P., Vogt S. S., Fischer D., Lissauer J. J., 1998, *ApJ*, 505, 147
- Marcy G. W., Butler R. P., Fischer D., Vogt S. S., Lissauer J. J., Rivera E. J., 2001, *ApJ*, 556, 296
- Masset F. S., Morbidelli A., Crida A., Ferreira J., 2006, *ApJ*, 642, 478
- Matsuo T., Shibai H., Ootsubo T., Tamura M., 2007, *ApJ*, 662, 1282
- Menou K., Goodman J., 2004, *ApJ*, 606, 520
- Miguel Y., Brunini A., 2009, *MNRAS*, 392, 391
- Miguel Y., Brunini A., 2010, *MNRAS*, 406, 1935
- Miguel Y., Guilera O., Brunini A., 2011, *MNRAS*, 412, 2113
- Mordasini C., Alibert Y., Benz W., 2009, *A&A*, 501, 1139
- Murray N., Chaboyer B., Arras P., Hansen B., Noyes R. W., 2001, *ApJ*, 555, 801
- Nelson R. P., Papaloizou J. C. B., 2004, *MNRAS*, 350, 849
- Paardekooper S.-J., Baruteau C., Crida A., Kley W., 2010, *MNRAS*, 401, 1950
- Pinsonneault M. H., DePoy D. L., Coffee M., 2001, *ApJ*, 556, 59
- Raymond S. N., O'Brien D. P., Morbidelli A., Kaib N. A., 2009, *Icarus*, 203, 644
- Rivera E. J. et al., 2005, *ApJ*, 634, 625
- Rivera E. J., Laughlin G., Butler R. P., Vogt S. S., Haghighipour N., Meschiari S., 2010, *ApJ*, 719, 890
- Sadakane K., Ohkubo M., Takeda Y., Sato B., Kambe E., Aoki W., 2002, *PASJ*, 54, 911
- Safronov V., 1969, *Evolution of the Protoplanetary Cloud and Formation of the Earth and Planets*. Nauka Press, Moscow
- Santos N. C., Israelian G., Mayor M., 2001, *A&A*, 373, 1019
- Santos N. C., Israelian G., Mayor M., Rebolo R., Udry S., 2003, *A&A*, 398, 363
- Santos N. C., Israelian G., Mayor M., 2004, *A&A*, 415, 1153
- Sozzetti A., Torres G., Latham D. W., Stefanik R. P., Korzennik S. G., Boss A. P., Carney B. W., Laird J. B., 2009, *ApJ*, 697, 544
- Stevenson D. J., 1982, *Planet. Space Sci.*, 30, 755
- Tanaka H., Takeuchi T., Ward W., 2002, *ApJ*, 565, 1257
- Thommes E. W., Duncan M. J., Levison H. F., 2003, *Icarus*, 161, 431
- Thommes E. W., Matsumura S., Rasio F. A., 2008, *Sci*, 321, 814
- Toomre A., 1964, *ApJ*, 139, 1217
- Veras D., Crepp J. R., Ford E. B., 2009, *ApJ*, 696, 1600
- Vinkovic D., 2006, *ApJ*, 651, 906
- Vogt S. S., Butler R. P., Marcy G. W., Fischer D. A., Henry G. W., Laughlin G., Wright J. T., Johnson J. A., 2005, *ApJ*, 632, 638
- Ward W. R., 1997, *Icarus*, 126, 261
- Weidenschilling S. J., Spaute D., Davis D. R., Marzari F., Ohtsuki K., 1997, *Icarus*, 128, 429
- Wright J. T., Upadhyay S., Marcy G. W., Fischer D. A., Ford E. B., Johnson J. A., 2009, *ApJ*, 693, 1084

This paper has been typeset from a  $\text{\TeX}/\text{\LaTeX}$  file prepared by the author.